Flexibility of Generator and Converter

Testing of Control System for Grid Connected Frequency Converter

HydroFlex

Increasing the value of hydropower through increased flexibility

Deliverable 4.7 Testing of Control System for Grid Connected Frequency Converter

Work package	WP4 Flexibility of Generator and Converter
Task	Task 4.4 Enhanced insulation winding insulation system and performance testing
Lead beneficiary	Norwegian University of Science and Technology - NTNU
Authors	Roy Nilsen, Thomas Haugan, Raghbendra Tiwari
Due date of deliverable	30.04.2022
Actual Submission date	27.04.2022
Type of deliverable	Report
Dissemination level	Public

This project has received funding from the European Union's Horizon 2020 research and innovation programme under grant agreement No 764011.

Executive Summary

At NTNU, a 100 kW laboratory setup with an Emulator of Reversible Pump Turbine has been developed in the Smart Grid Lab. An Induction Motor Drive with an Active Front End (AFE) at input stage is used for emulation of the Reversible Pump Turbine including a Speed Governor. A special designed 100 kVA Synchronous Machine is connected to the grid via a full power frequency converter with an AFE as grid connected converter. This large project has been a co-operation between 3 different projects/sources:

- AVIT-funding from NTNU for financing of the hardware set-up: 2 MNOK
- The FME HydroCen project has financed the work of a PhD-student and the work of SINTEF with the Turbine Emulator including the Induction Motor Drive.
- HydroFlex has financed the development of the completed Synchronous Motor Drive, including use of communication system as CAN and fiberlink.

Even though the focus of the activities financed by HydroFlex is the Synchronous Motor drive, a short description of the total system is presented.

A complete control system for a Synchronous Motor Drive has been developed in this HydroFlex project. To accelerate the SW development, an embedded real time emulator of the converter, motor and load was implemented in a Field Programmable gate Array (FPGA) of Zynq7030 System on Chip (SoC) from Xilinx.

As a second step, the SW was successfully tested on the real 100 kVA drive system in the Smart Grid Lab at NTNU. Some minor adjustments were made to adapt to the actual setup. A DC-link voltage controller for synchronous motor drive was developed and successfully tested.

As a final step the SM drive was tested together with the Induction Motor Drive running as a Reversible Pump Turbine load emulator. The IM Drive was controlled from the Opal RT. Both pump operation and turbine operation were tested succesfully. Tests including mode switching, i.e. from pump to turbine and from turbine to pump operation, were executed. Even Low Voltage Ride Through was tested.

The conclusion is that the goals of the project have been accomplished.

Table of Contents

Abbreviations

AD	Analog to digital converter
AFE	Active Front End converter
DC	Direct Current
FPGA	Field Programmable Gate Array
IGBT	Insulated Gate Bipolar Transistor
IM	Induction Machine
LCL	Filter with inductance, capacitor and a second inductance
Opal RT	Opal Real Time system
PI	Proportional and Integral controller
PLC	Programmable Logic Controller
RPT	Reversible Pump Turbine
SM	Synchronous Machine
SW	SoftWare

1 Introduction

At NTNU, a 100 kW laboratory setup with an Emulator of Reversible Pump Turbine has been developed in the Smart Grid Lab. An Induction Motor Drive with an Active Front End (AFE) at input stage is used for emulation of the Reversible Pump Turbine including a Speed Governor. A special designed Synchronous Machine is connected to the grid by help of a full power frequency converter with an AFE as grid connected converter. The set-up is shown in Figure 1.0.1.

This large project has been a co-operation between 3 different projects/sources:

- AVIT-funding from NTNU for financing of the hardware set-up: 2 MNOK
- The FME HydroCen project has financed the work of a PhD-student and the work of SINTEF with the Turbine Emulator including the Induction Motor Drive.
- HydroFlex has financed the development of the completed Synchronous Motor Drive, including use of communication system as CAN and fiberlink.

Even though the focus of the activities financed by HydroFlex is the Synchronous Motor drive, a short description of the total system is presented. The total system is very similar to the system discussed in [1].

The main parts of this report are the description of SW development of the SM drive by help of an Emulator in the FPGA, the implementation of the real SM drive and finally the complete system test.

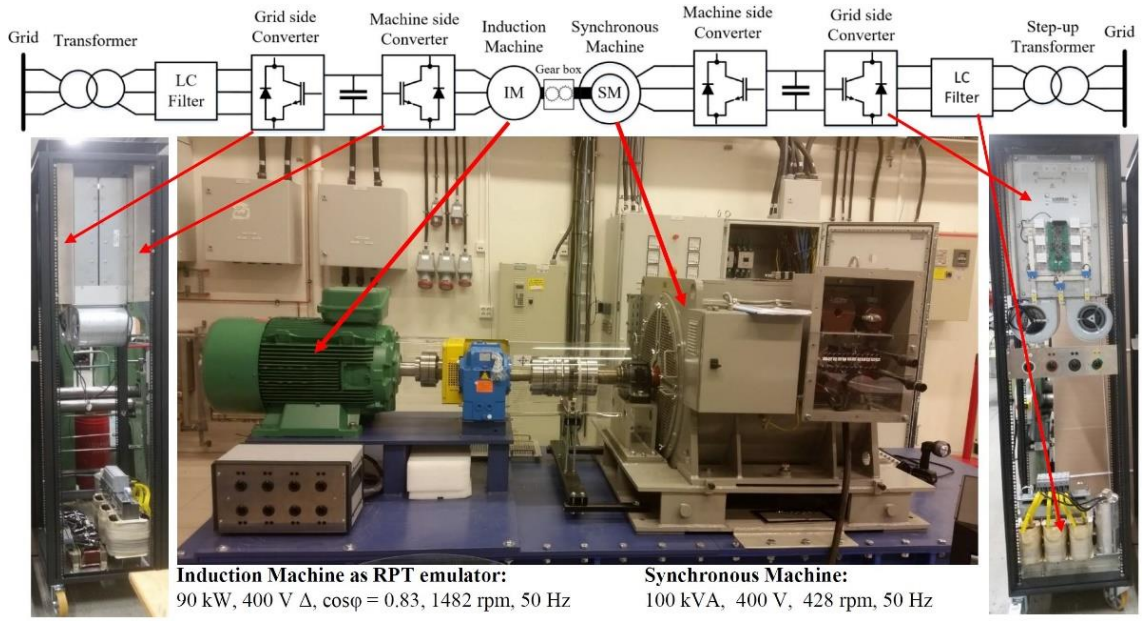

Figure 1.0.1: Overview of the Reversible Pump Turbine Emulator

2 System Description

The total drive system is shown in Figure 2.0.1. The Induction Motor Drive is used as the RPT Emulator. The converters are based on 180 kW Semikron SEMIKUBE Frame SL40. The control boards are based on Avnet picoZed board and an interface board developed by SINTEF. The SystemOnChip (SoC) used on the Avnet board is the Zynq 7030 from Xilinx with 2 Floating point processors and one FPGA in one chip. The control board can control two 2-level 3-phase converters and is equipped with an 8 channel AD-converter. Three output currents and the dc-link voltage are measured in each converter.

In principle the control board for the SM inverter could control even the exciter. However, to be able to connect the SM directly to the AC-grid without the full power converter it was decided to have a separate control board for the exciter converter. This means that when full power converter is used, the exciter control board will be in slave mode and controlled from the SM inverter control board. The communication channel is CAN. This will introduce some delay in the control of the field current.

The Opal RT is used both as a SCADA system and for emulating the waterway, turbine, guide vane model and the turbine speed controller (governor). The communication channel to the control boards are optical High Speed Serial links, except to the SM inverter where ModBus TCP/IP is used.

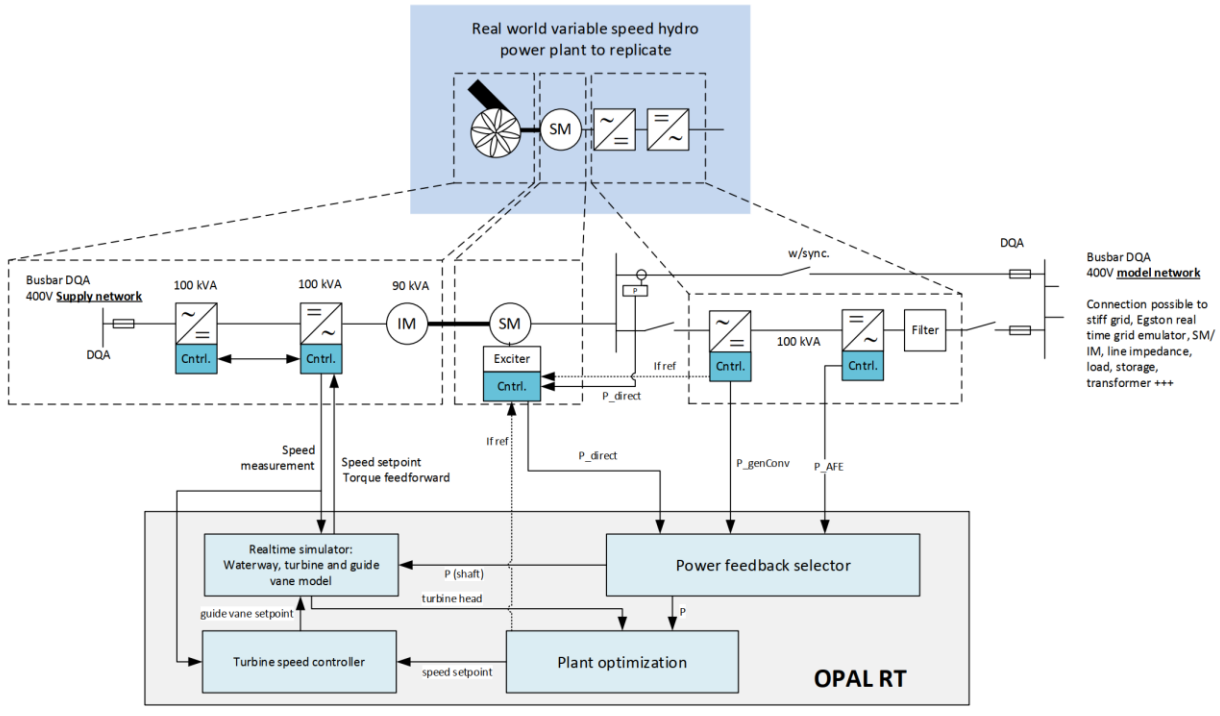

Figure 2.0.1: Complete Drive System with Opal RT [2]

2.1. Control Structure

2.1.1 Opal RT as High Level Plant Controller

The Opal RT is used as a Plant Controller. This means that secondary and tertiary control level can be implemented here. It is also the Opal RT which decides the operation mode of the plant. Two different modes are implemented: Turbine Mode and Pump Mode. It is also the Opal RT which control the mode switching.

Turbine Mode

In Turbine mode the Emulator is in ordinary Speed Control Mode by help of the governor controlling the guide vane opening. The SM inverter is in DC-link Control Mode. This means that the motor torque is controlled by a DC-link controller responsible for keeping the DC-link voltage at its reference value. The optimal speed reference of the governor can be calculated based on the power from the inverter into the DC-link. The AFE converter connected to the grid can be either in grid following mode or grid generating mode. In grid following mode the AFE is synchronized to the grid and deliver active and reactive power according to the refence values. It can be in voltage droop control if required. In grid generating mode the AFE is in voltage- and frequency droop control including emulating virtual damping and inertia.

Pump Mode

In Pump mode the Emulator is controlling the guide vane opening directly and usually in fixed position during ordinary operation. During mode switching, however, it can be controlled to reduce the required torque from the SM when passing zero speed. The SM inverter is then in Speed Control Mode. The AFE converter is now in DC-link voltage control mode. The reactive power can be controlled to support voltage control if the converter rating allows this.

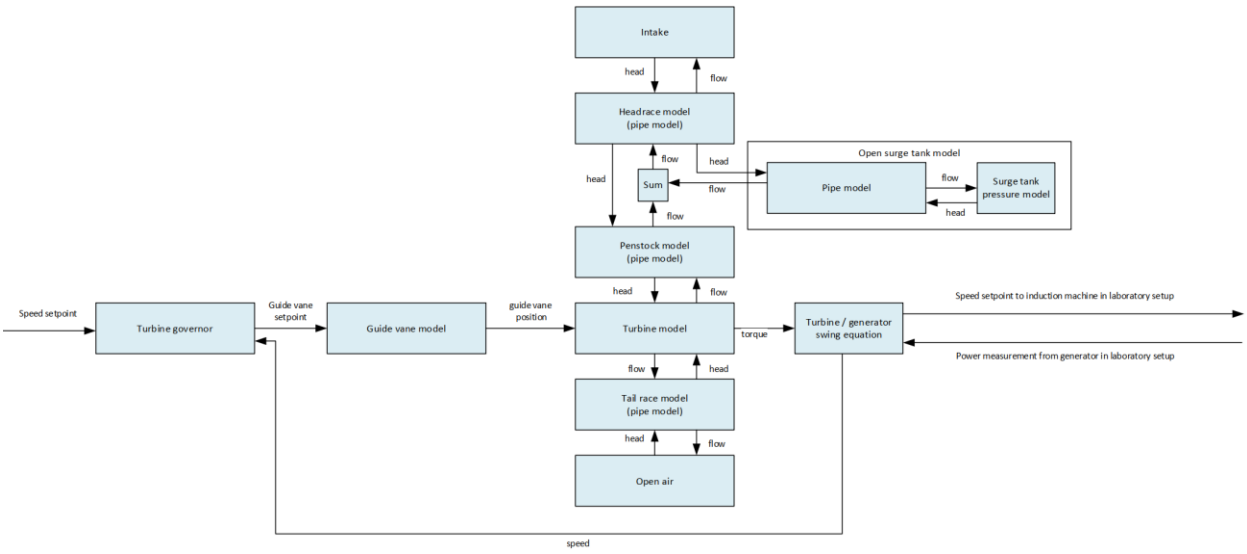

Figure 2.0.2: Emulator implemented in Opal RT [2]

2.1.2 Opal RT as emulator

The shaft torque of the induction motor shall emulate the torque on the shaft of a RPT. The emulation of the waterway, turbine and guide vane control can be implemented either in the motor controller or the Opal RT. In this set-up it is implemented in the Opal RT. The programming is made in Simulink.

Different models for the emulator are implemented, but the basic idea is the emulate a turbine torque at the shaft. The signal protocol is shown in Figure 2.0.3.

2.2. Induction Motor Drive

2.2.1 AFE converter

This AFE is always in DC-link voltage Control Mode. The communication between the Opal RT and the AFE goes via the IM Drive (see below).

This AFE also has a LCL-filter between the converter and the grid, as shown in Figure 2.0.1.

2.2.2 Induction Motor Control

The induction motor is controlled from the Opal RT and is either in speed- or torque control mode. The signals transferred to and from the IM drive is shown in Figure 2.0.4. As we understand the AFE control board is in slave mode and controlled via the Motor Inverter Control board. An interlock mechanism is introduced, such that the motor inverter is disabled until the AFE is up running.

From:- OPAL To:- Pump-turbine Emulator

S.N.	Signal	Signal type	Min value	Max value	Scaling	Purpose

From:- Pump-turbine Emulator To:- OPAL

S.N.	Signal	Signal type	Min value	Max value	Scaling	Purpose
1	Status word					To know the status
2	Control Mode					Pump / turbine
3	Torque ref (N.m)					Load torque ref (to be forwarded to IM drive) in pump mode
4	Speed ref (rpm)					Speed ref (to be forwarded to IM drive) in turbine mode
5	Guide vane opening (degree/percent)					
6	Flow (m3/s)					
7	Upper surge tank elevation (m)					To check during dynamics
8	Lower surge tank elevation (m)					
9	Net head (m)					

Figure 2.0.3: Signal protocol between Opal RT High Level Controller and Opal RT Pump-Turbine Emulator

From:- OPAL	To:- IM Drive					
S.N.	Signal	Signal type	Min value	Max value	Scaling	Purpose
1	Start Stop command					start stop of the AFE converter
2	Drive Control Mode					Torque control / speed control
3	Torque Ref					
4	Speed Ref					

From:- IM Drive	To:- OPAL					
S.N.	Signal	Signal type	Min value	Max value	Scaling	Purpose
	Status word					To know the status
	Control Mode					Actual mode - Torque control /Speed control
	Torque (N.m)					Actual torque output
	Speed (rpm)					Actual speed of the machine
	Current (A)					Measured output current from the converter
	Active Power (kW)					Output power from the converter
	Reactive Power (kVAr)					Reactive power from the converter
	Dc link voltage (V)					Actual dc-link voltage

Figure 2.0.4: Signal protocol between Opal RT and IM Drive

2.3. Synchronous Motor Drive

2.3.1 AFE converter

This AFE is either in DC-link voltage Control Mode or Active Power Control/Frequency droop control. The last degree of freedom can be used for reactive power/voltage droop control.

No interlock between motor inverter and the AFE is present. This means that the motor inverter can be started to charge the dc-link even if the AFE is not started.

The signal protocol is presented in Figure 2.0.6.

2.3.2 Synchronous Motor Control

The main focus of the HydroFlex project with respect to this setup has been to develop and test the SM drive Control.

Two converters are used in the SM Drive; stator inverter and the exciter converter. The first one is a classical 2-level 3-phase inverter, while the last one is chosen to be a H-bridge converter with a 6-pulse diode rectifier as input. In addition, a brake chopper is included.

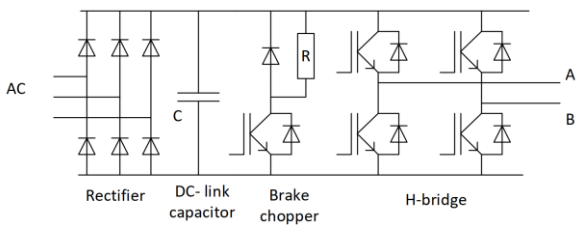

Figure 2.0.5: Exciter Converter [3]

From:- OPAL	To:- SM Drive					
S.N.	Signal	Signal type	Min value	Max value	Scaling	Purpose
1	Control Word	UINT	0	0xFFFF		start & stop the drive
2	Drive Control Mode Request	UINT				To make the drive run in torque/speed/dc-link control mode
3	Power max (kW)	INT				
4	Power min (kW)	INT				
5	Power Ref (kW)	INT				
6	UdcLink Ref [V]	INT				
7	Torque Ref [Nm]	INT				
8	Speed Ref [rpm]	INT				
2	AFE Control Relay	UINT				

From:- SM Drive	To:- OPAL					
S.N.	Signal	Signal type	Min value	Max value	Scaling	Purpose
1	Status Word	UINT				To know the status
2	Warning Word	UINT				
3	Fault Word	UINT				
4	Limit Word	UINT				
5	Application State	UINT				
6	Actual Control Mode	UINT				Torque/speed/dclink control mode
7	Active Converter Power (kW)	INT				Output power from the converter
8	Reactive Converter Power In (kVAr)	INT				Reactive power from the converter
9	Current (A)	INT				Measured output current from the converter
10	Dc link voltage (V)	INT				Actual dc-link voltage
11	Torque Ref Used (N.m)	INT				Torque Referenced used after limitation
12	Torque Actual (N.m)	INT				Torque produced by machine (calculated)
13	Torque Limit Max Used (N.m)	INT				Max Torque Limit
14	Torque Limit Min Used (N.m)	INT				Min Torque Limit
15	Speed (rpm)	INT				Actual speed of the machine
16	Shaft Power (kW)	INT				Estimated output Power
	Speed Ref Turbine [rpm]					

From:- OPAL	To:- AFE (SM)					
S.N.	Signal	Signal type	Min value	Max value	Scaling	Purpose
1	Start Stop command					start stop of the AFE converter
2	Drive Control Mode					Dc link voltage control / AC frequency control
3	Frequency reference (or equivalent)					To control the power out of the converter to the grid

From:- AFE (SM side)	To:- OPAL					
S.N.	Signal	Signal type	Min value	Max value	Scaling	Purpose
1	Status word					To know the status
2	Control Mode					Actual mode - Dc link voltage control / AC frequency control
3	Current (A)					Measured output current from the converter
4	Active Power (kW)					Output power from the converter
5	Reactive Power (kVAr)					Reactive power from the converter
6	Dc link voltage (V)					Actual dc-link voltage

Figure 2.0.6: Signal protocol between Opal RT and SM Drive & AFE

The exciter converter is designed with 600 V IGBTs and a 350 V dc-link voltage. The rated exciter voltage is only 20 V and the current is 120 A. The dc-link voltage used is 50 V only.

The transformer rating is 8 kVA.

3 Synchronous Motor Drive Development

In the Power Electronic Systems and Components (PESC) and the Department of Electric Power Engineering (IEL) at NTNU, we have developed a PESC Control Platform for internal use by Master and PhD-students. The platform is based on a SINTEF interface board and a picoZed board from Avnet. The picoZed board is equipped with a Zynq7030 chip. This chip has 2 floating point processors and one Field Programmable Gate Array. The use of the components is as follow:

- Processor 0 is used for communication and up-loading of SW releases etc.
- Processor 1 is used entirely for the motor control (drives control: motor, AFE, dc-dc)
- The FPGA is used for filters, PWM, protection, reading AD-converters, DA-converter control, resolver/encoder interface, relay control, emulators, etc.

The board is communicating with our PC or a PLC/Opal RT via an Ethernet connector. The board is also equipped with 4 optical transceivers for fast communication with the other boards. These transceivers are used for communication with the Opal RT for some of the control boards. The Ethernet plug is used for communication via ModBus or directly to a PC. A combination of router and switch is used in the lab-setup.

In the final SM drive a CAN-bus interface is used for communicating with the control board of the exciter converter. In future solutions this can be done by help of the optical fiber link.

During Covid the access to the lab was restricted. To speed up the development an emulator of converters, motor and load (Newton 2nd law) was implemented in the FPGA. In emulator mode the PMW signals are disabled from the real inverter and directed to the emulator. The AD-measurements are then connected to the emulator instead of the real AD-converter. The emulator has an output module with 13-bit resolution and the same V/bit and A/bit as the real AD-converter.

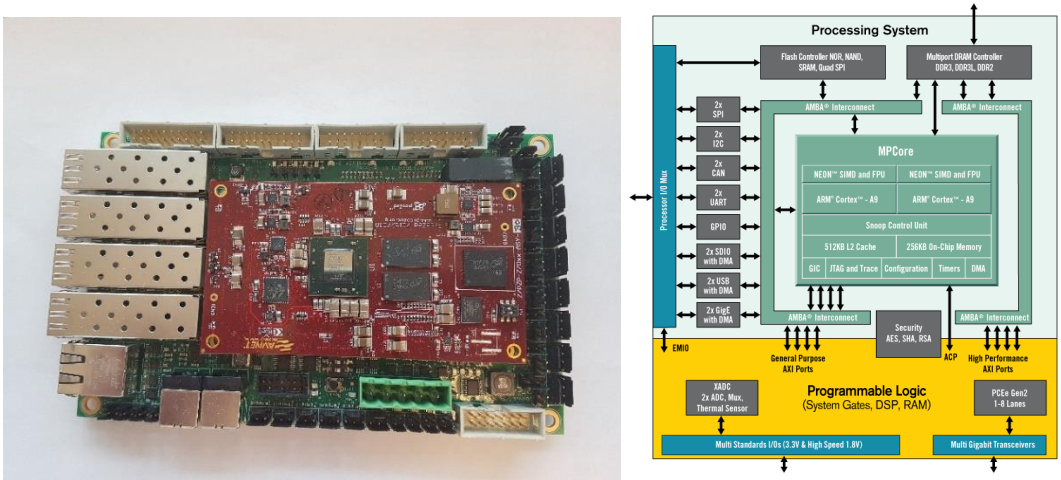

Figure 3.0.1:SINTEF board, picoZed board and overview of the Zynq chip

3.1 SW structure

The complete drive software is implemented in processor 1. The structure of the SW is very modular as shown in Figure 3.2. The concept is based on the "need-to-know" basis. This means that the Application Layer do not know, which type of motor is used. For the application Layer the Drive Layer is only a torque actuator. In the same way the Drive Layer do not know whether the converter is 2-level or 3-level converter; it only requests a voltage vector amplitude and angle.

It is in the *Application Layer* where the communication with upper control systems as PLC, Opal RT, panel or PC is implemented. In addition, it is in this layer the main state machine of the drive is implemented. In the run-state, different control modes can be chosen. The most important modes are torque control, speed control, power control, DC-link voltage control and Load Emulator mode. The routines are implemented such that one can switch between control modes on the fly without instant transients in the torque reference. Also reference filters are implemented. The output from the Application Layer to the Drive Layer is the torque reference. Several feedback signals can be read from the Drive Layer. Typical values are actual speed, actual reference used and actual upper and lower torque limits. The Application Layer can also send a request-command to the Drive Layer state machine about going to a given state.

It is in the *Drive Layer* the real torque control is executed, i.e. the motor control is implemented. The structure is very similar for all type of machines, but some functions have to be adapted to the actual type of motor. The first part is the torque limiter chain; over/under speed limiter, power limiter, max/min torque limiter, DC-link under/over voltage limiter and current limiters. Also torque pull-out limiter is implemented. In addition, the flux controller including field-weakening function is implemented. Optimal torque control is also implemented. This function is different for different type of machines. Based on the torque command and the flux controller, the references for stator currents are calculated. For SM also the field current reference value has to be calculated as well. Finally, in the case of SM drive, the 3 current controllers calculate the required voltages; one voltage vector for the stator inverter and a DC-voltage for the exciter converter. The requested voltage vectors are sent to the converter Layer (one for each converter). Measured currents and voltages from each converter can be read by the Drive Layer. Also, information about status/faults can be read.

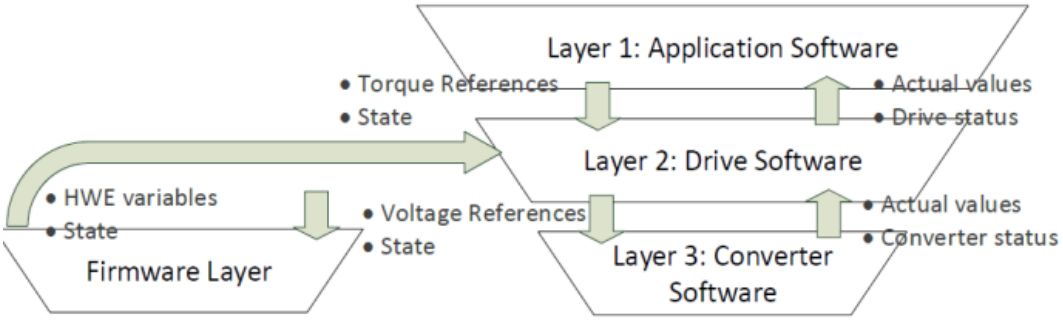

Figure 3.2: SW structure of the SM drive

The state machine of the *Converter Layer* is controlled by the Drive Layer. It is only 2 states to be discussed here; disable state and enable state. In disable state, the pulses to the IGBTs are disabled. In the enable state, the PWM modulator is in operation, but also current hysteresis controllers can be chosen. For the SM drive, PMW modulator with asymmetrical switching and 3rd harmonic injection is implemented. It is thus the Converter Layer which is communicating with the IP Cores in the FPGA related to the Converter control, protection and measurements. The communication is made via the AXI-bus interface.

Communication routines for other IP Cores in the FPGA not related to the Converters, are implemented in the *FirmWare Layer*. Typical functions are encoder readings, control of relays, digital I/O signal, etc. In addition, the Load Emulator is implemented in this Layer. The Load Emulator functions can be used in two ways; as load in the FPGA Drive Emulator or as torque reference in the Application Layer in Load Emulator mode. The first application is of interest when developing the motor software, while the other application is when you are going to emulate a load in the lab in a back-to-back setup. In our case, we will use the Opal RT for load emulation.

3.2 Functions implemented in the FPGA

The main parts of the FPGA program discussed in this report are the Converter FirmWare and the Drive Emulator.

3.2.1 Converter FirmWare

The sub-circuit for the Converter FPGA design is presents in Figure 3.3. The AXI-bus interfaces to the processor are indicated by + -sign, while the ordinary pins are connections to other IP-cores inside the FPGA-design.

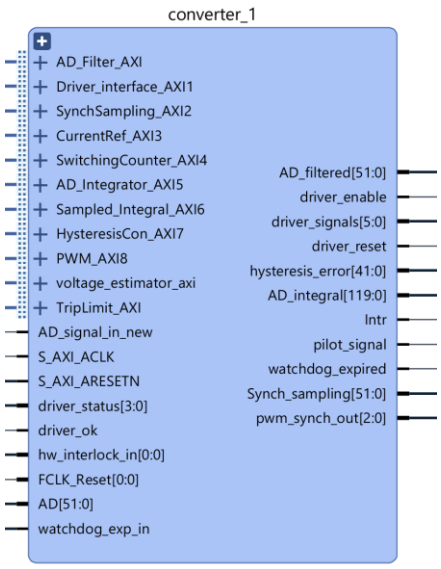

Figure 3.3: Converter Sub-circuit in the Vivado FPGA design

Typical functions implemented in this converter module are PWM-modulator and protection function tripping the drive for over-currents or overvoltage in the DC-link. In addition, different types of filters are implemented. The AD-converter sampling rate is in the MHz-range. It is also the PWM-modulator which gives the interrupt for the controller. Asymmetrical switching is used, which the means that an interrupt is generated at the top and bottom of the triangular wave carrier.

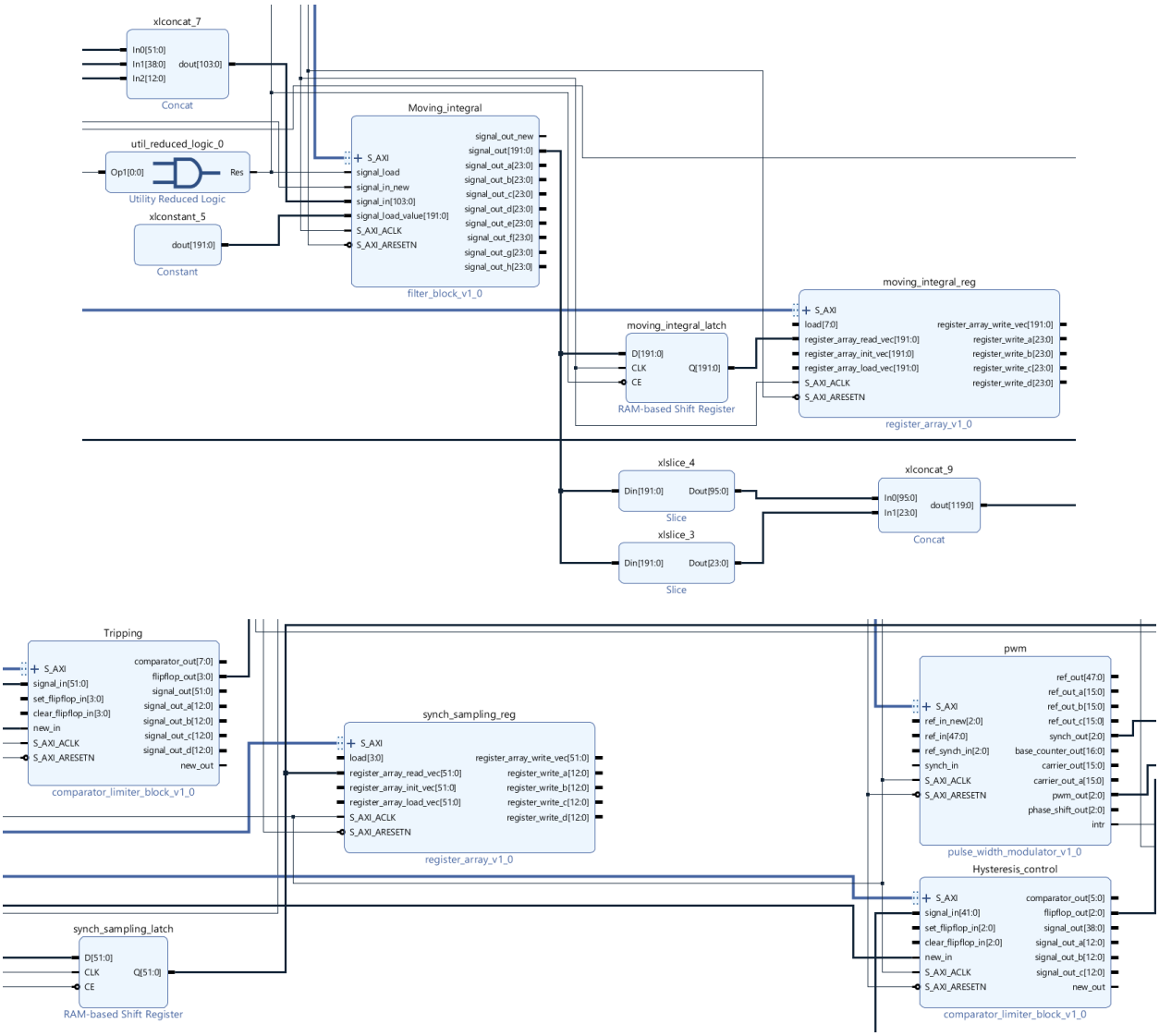

Figure 3.4: Some parts of the Converter Sub-circuit

3.3.2 Drive Emulator

The basic idea for implementation of a Drive Emulator in the FPGA was to be able to do most of the SW development for the drive only by help of the control board. This enabled us to develop most of our drive SW and some FPGA IP cores in our office without access to the actual drive.

In the Emulator, two 3-phase 2 level converters are modelled. The converters are modelled with ideal switches. When no gate signals are given, the potential of the actual bridge leg output is given by the sign of the output current, i.e. the ideal diodes are conducting. In this first version of the emulator the DC-link voltages are constant. This means that the DC-link voltage controller could not be tested in the emulator, but only in the real drive set-up.

The motor model is implemented in the dq-frame. This means that the input voltages from the converter have to be transformed to the dq-frame. The electrical rotor position is used. This position is calculated based on the mechanical angle in the emulator and the number of pole pairs of the machine. Newtons 2nd law for rotational movements, i.e. torque and speed, is implemented. All models are implemented in per unit (pu). The conversion to Ampere and Volt is made in the circuit emulating the 12 bit AD-converters. This 13 bit integer number has the same A/bit or V/bit as the real AD-converter. This means that the FPGA IP cores do not observe much difference between Emulator or real AD-converter feedback.

The angle and speed feedback to the controller are the synchronized sampled 32-bit values in the FPGA. This means that the resolution of these variables in general are more accurate than in the real drive.

Variables in the FPGA are usually 32 bit, while the scaling is such that the pu variables can be in the range of +7.99 to -8 pu. The resolution pr. bit is then 3.725x10^{-9}. For the integrator in the model a 64 bit resolution is used. To limit the word length, the motor model is implemented with a time step of 1 µs. The converter, however, operates with the time resolution of the FPGA clock equal 10 ns. Especially the integrators will be dependent on the time resolution; reduced time step T_{step} requires more bits.

Clock	Frequency	Time step
FPGA Clock	100 MHz	T_{FPGA} = 10 ns
Processor interrupt cycle	8 kHz	T_{samp} = 125 µs
Solver clock	1 MHz	T_{step} = 1 µs

Figure 3.5: Clock settings in the Drive Emulator

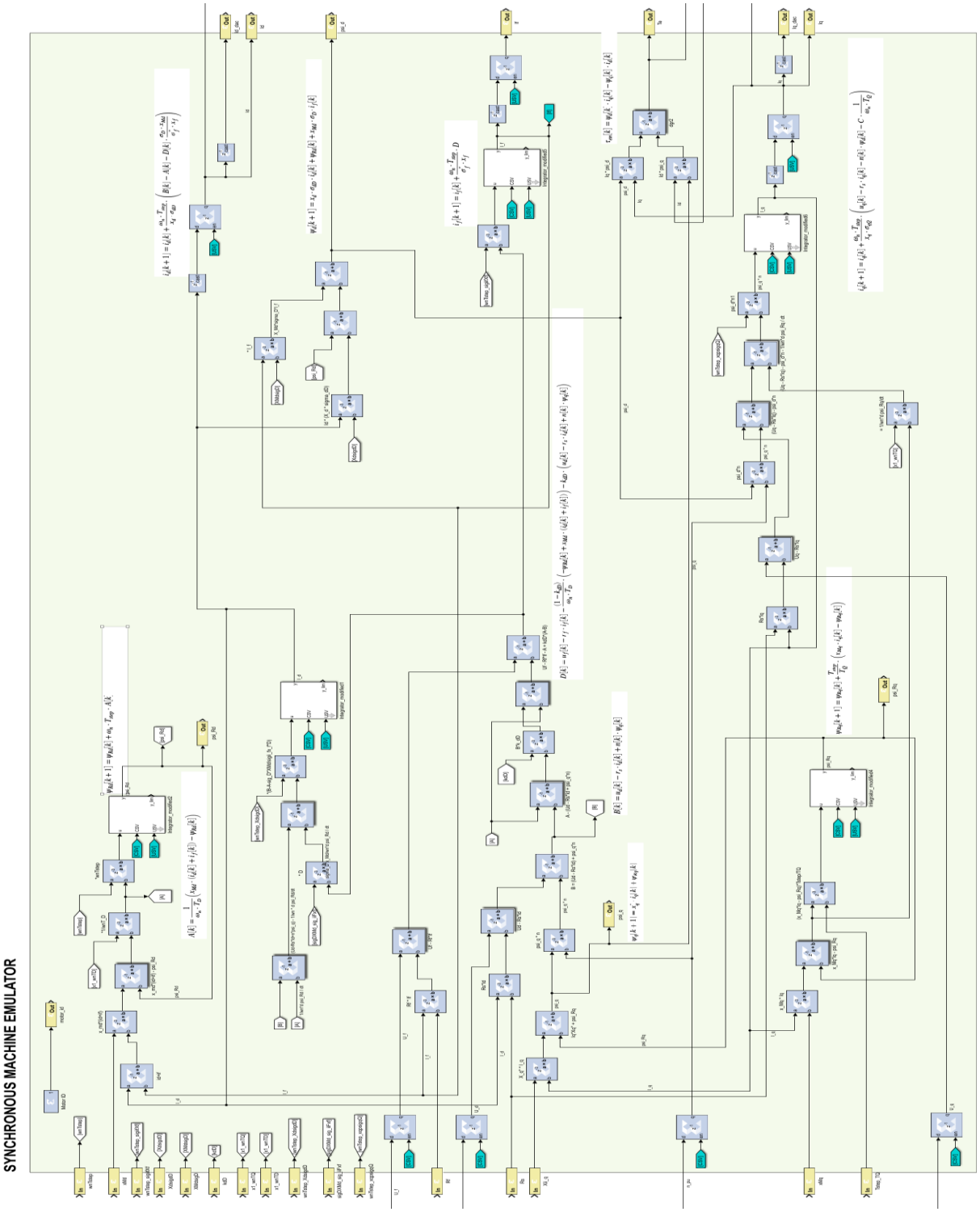

Figure 3.6: Simulink schematic of the Synchronous Machine Emulator

3.3 Motor Model

The mathematical model of the synchronous machine chosen, depend on the purpose of the model. In the emulator, the model with the flux linkages as state variables can be chosen. This model is in pu as follows:

$$u_d = r_s \cdot i_d + \frac{1}{\omega_n} \cdot \frac{d\psi_d}{dt} - n \cdot \psi_q \qquad u_q = r_s \cdot i_q + \frac{1}{\omega_n} \cdot \frac{d\psi_q}{dt} + n \cdot \psi_d$$

$$u_0 = r_s \cdot i_0 + \frac{1}{\omega_n} \cdot \frac{d\psi_0}{dt} \qquad u_f = r_f \cdot i_f + \frac{1}{\omega_n} \cdot \frac{d\psi_f}{dt}$$

$$0 = r_D \cdot i_D + \frac{1}{\omega_n} \cdot \frac{d\psi_D}{dt} \qquad 0 = r_Q \cdot i_Q + \frac{1}{\omega_n} \cdot \frac{d\psi_Q}{dt}$$

$$\psi_d = x_d \cdot i_d + x_{md} \cdot i_f + x_{md} \cdot i_D \qquad \psi_q = x_q \cdot i_q + x_{mq} \cdot i_Q$$

$$\psi_0 = x_{s\sigma} \cdot i_0$$

$$\psi_f = x_{md} \cdot i_d + x_f \cdot i_f + x_{md} \cdot i_D$$

$$\psi_D = x_{md} \cdot i_d + x_{md} \cdot i_f + x_D \cdot i_D \qquad \psi_Q = x_{mq} \cdot i_q + x_Q \cdot i_Q$$

The flux linkage equations can be solved for calculation of the currents. This model is convenient when saturation phenomena and magnetic cross-coupling effects should be taken into account. The inductances can be expressed by help of mutual inductances and the leakage inductances as:

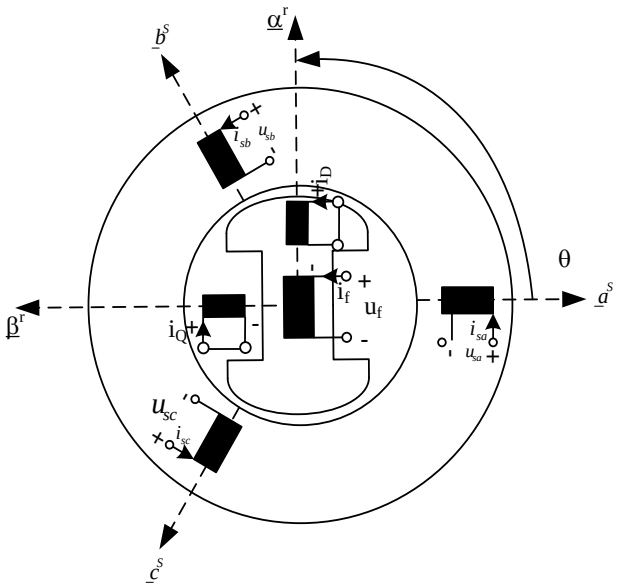

Figure 3.7: Classical 3-phase Synchronous Machine

$$x_d = x_{md} + x_{s\sigma} \qquad x_D = x_{md} + x_{D\sigma} \qquad x_f = x_{md} + x_{f\sigma} \quad x_q = x_{mq} + x_{s\sigma} \qquad x_Q = x_{mq} + x_{Q\sigma}$$

The torque equation for the mechanical system can be expressed as:

$$\tau_e = \quad \psi_d \cdot i_q - \quad \psi_q \cdot i_d$$

$$T_m \cdot \frac{dn}{dt} = \tau_e - \tau_L \qquad \frac{\mathrm{d}\theta}{\mathrm{dt}} = \omega_n \cdot n \qquad \theta_{\mathrm{mech}} = \theta / \ p$$

However, for developing the control strategy and choice of control parameters, another version of the model might give better physical insight. By choosing the stator currents, field currents and damper winding flux linkages as state variables, the model becomes:

$$u_d = r_d^{''} \cdot i_d + \frac{x_d^{''}}{\omega_n} \cdot \frac{di_d}{dt} - \frac{r_{Rd}^{'}}{x_{Md}} \cdot \psi_{Rd} + r_{Rd}^{'} \cdot i_f + k_{fD} \cdot \left(u_f - r_f \cdot i_f\right) - n \cdot \psi_q$$

$$u_q = r_q^{''} \cdot i_q + \frac{x_q^{''}}{\omega_n} \cdot \frac{di_q}{dt} - \frac{r_{Rq}}{x_{Mq}} \cdot \psi_{Rq} + n \cdot \psi_d$$

$$u_f = r_f^{''} \cdot i_f + \frac{x_f^{''}}{\omega_n} \cdot \frac{di_f}{dt} - \frac{r_{Rd}^{''}}{x_{Md}} \cdot \psi_{Rd} + r_{Rd}^{''} \cdot i_d + k_{dD} \cdot \left(u_d - r_s \cdot i_d + n \cdot \psi_q\right)$$

$$T_D \cdot \frac{d\psi_{Rd}}{dt} = \ -\psi_{Rd} + x_{Md} \cdot \left(i_d + i_f\right)$$

$$T_Q \cdot \frac{d\psi_{Rq}}{dt} = \ -\psi_{Rq} + x_{Mq} \cdot i_q$$

The flux linkages can be expressed as:

$$\psi_d = \psi_{Rd} + \sigma_{dD} \cdot x_d \cdot i_d + \sigma_D \cdot x_{Md} \cdot i_f \qquad \psi_q = \psi_{Rq} + \sigma_{qQ} \cdot x_q \cdot i_q$$

$$\psi_f = \psi_{Rd} + \sigma_{Df} \cdot x_f \cdot i_f + \sigma_D \cdot x_{Md} \cdot i_d$$

The parameters and flux linkages are defined as:

$$\psi_{Rd} = \frac{\psi_D}{1+\sigma_D} \qquad \psi_{Rq} = \frac{\psi_Q}{1+\sigma_Q} \qquad \mathrm{T}_D = \frac{x_{Md}}{\omega_n \cdot r_{Rd}} \qquad \mathrm{T}_Q = \frac{x_{Mq}}{\omega_n \cdot r_{Rq}}$$

$$r_{Rd} = \frac{r_D}{\left(1+\sigma_D\right)^2} \qquad r_{Rq} = \frac{r_Q}{\left(1+\sigma_Q\right)^2} \qquad x_{Md} = \frac{x_{md}}{1+\sigma_D} \qquad x_{Mq} = \frac{x_{mq}}{1+\sigma_Q}$$

$$r_{Rd}^{'} = \frac{r_D}{\left(1+\sigma_D+\frac{\sigma_D}{\sigma_f}\right) \cdot \left(1+\sigma_D\right)} \qquad r_{Rd}^{''} = \frac{r_D}{\left(1+\sigma_D+\frac{\sigma_D}{\sigma_d}\right) \cdot \left(1+\sigma_D\right)}$$

The leakage coefficients are defined as:

$$\sigma_{dD} = 1 - \frac{1}{(1+\sigma_d)\cdot(1+\sigma_D)} \qquad \sigma_{Df} = 1 - \frac{1}{(1+\sigma_f)\cdot(1+\sigma_D)} \qquad \sigma_{qQ} = 1 - \frac{1}{(1+\sigma_q)\cdot(1+\sigma_Q)}$$

$$\sigma_d^{''} = 1 - \frac{1}{(1+\sigma_d)\cdot\left(1+\frac{\sigma_f\cdot\sigma_D}{\sigma_f+\sigma_D}\right)} \qquad \sigma_f^{''} = 1 - \frac{1}{(1+\sigma_f)\cdot\left(1+\frac{\sigma_d\cdot\sigma_D}{\sigma_d+\sigma_D}\right)}$$

$$x_d^{''} = \sigma_d^{''}\cdot x_d \qquad x_f^{''} = \sigma_f^{''}\cdot x_f \qquad x_q^{''} = \sigma_{qQ}\cdot x_q$$

$$r_d^{'} = r_s + \frac{r_D}{(1+\sigma_D)^2} \qquad r_f^{'} = r_f + \frac{r_D}{(1+\sigma_D)^2} \qquad r_q^{'} = r_s + \frac{r_Q}{(1+\sigma_Q)^2}$$

$$r_d^{''} = r_s + (1-k_{fD})\cdot\frac{r_D}{(1+\sigma_D)^2} = r_s + \frac{r_D}{\left(1+\sigma_D+\frac{\sigma_D}{\sigma_f}\right)\cdot(1+\sigma_D)} \qquad k_{fD} = \frac{\sigma_D}{\sigma_f\cdot\left(1+\sigma_D+\frac{\sigma_D}{\sigma_f}\right)}$$

$$r_f^{''} = r_f + (1-k_{dD})\cdot\frac{r_D}{(1+\sigma_D)^2} = r_f + \frac{r_D}{\left(1+\sigma_D+\frac{\sigma_D}{\sigma_d}\right)\cdot(1+\sigma_D)} \qquad k_{dD} = \frac{\sigma_D}{\sigma_d\cdot\left(1+\sigma_D+\frac{\sigma_D}{\sigma_d}\right)}$$

This model has some similarities to the model usually applied for rotor flux-oriented control of Induction Machines, where the rotor flux linkage equation includes the large rotor time constant. It is also clear that in this model the large time constants are the damper winding time constants. The torque can be expressed as:

$$\tau_e = \psi_d\cdot i_q - \psi_q\cdot i_d = \psi_{Rd}\cdot i_q - \psi_{Rq}\cdot i_d + \left(\sigma_D\cdot x_{Md}\cdot i_f + \left(\sigma_{dD}\cdot x_d - \sigma_{qQ}\cdot x_q\right)\cdot i_d\right)\cdot i_q$$

As shown by the equations for the currents, fast stator current responses can be achieved due to small time constants. The damper winding flux linkages, however, have larger time constants. This will influence the torque response somewhat, which will be discussed later in this report. The dq-transformations used in this model are the classical Park-transformations:

$$\mathbf{T}_{ss}^{r} = \frac{2}{3}\cdot\begin{bmatrix} \cos\theta & \cos\left(\theta-\frac{2\pi}{3}\right) & \cos\left(\theta-\frac{4\pi}{3}\right) \\ -\sin\theta & -\sin\left(\theta-\frac{2\pi}{3}\right) & -\sin\left(\theta-\frac{4\pi}{3}\right) \\ \frac{1}{2} & \frac{1}{2} & \frac{1}{2} \end{bmatrix} \qquad \mathbf{T}_{ss}^{-r} = \left(\mathbf{T}_{ss}^{r}\right)^{-1} = \begin{bmatrix} \cos\theta & -\sin\theta & 1 \\ \cos\left(\theta-\frac{2\pi}{3}\right) & -\sin\left(\theta-\frac{2\pi}{3}\right) & 1 \\ \cos\left(\theta-\frac{4\pi}{3}\right) & -\sin\left(\theta-\frac{4\pi}{3}\right) & 1 \end{bmatrix}$$

A more classical model used for analysing the synchronous machine is the model based on transfer-functions, with the stator d- and q components and the field current as outputs:

$$u_d(s) = r_s \cdot i_d(s) + \frac{1}{\omega_n} s\psi_d(s) - n \cdot \psi_q(s) \qquad u_f(s) = r_f \cdot i_f(s) + \frac{1}{\omega_n} s\psi_f(s)$$

$$u_q(s) = r_s \cdot i_q(s) + \frac{1}{\omega_n} s\psi_q(s) + n \cdot \psi_d(s)$$

Where the flux linkages can be expressed as:

$$\psi_d(s) = x_d(s) \cdot i_d(s) - G(s) \cdot u_f(s) \qquad \psi_q(s) = x_q(s) \cdot i_q(s)$$

Here the transfer functions become:

$$x_d(s) = \frac{1 + (T_4 + T_5) \cdot s + T_4 \cdot T_6 \cdot s^2}{1 + (T_1 + T_2) \cdot s + T_1 \cdot T_3 \cdot s^2} \cdot x_d \approx \frac{(1 + T_d^{'} \cdot s) \cdot (1 + T_d^{''} \cdot s)}{(1 + T_{d0}^{'} \cdot s) \cdot (1 + T_{d0}^{''} \cdot s)} \cdot x_d$$

$$G(s) = \frac{1 + T_{D\sigma} \cdot s}{1 + (T_1 + T_2) \cdot s + T_1 \cdot T_3 \cdot s^2} \cdot \frac{x_{md}}{r_f} \approx \frac{1 + T_{D\sigma} \cdot s}{(1 + T_{d0}^{'} \cdot s) \cdot (1 + T_{d0}^{''} \cdot s)} \cdot \frac{x_{md}}{r_f}$$

$$x_q(s) = \frac{1 + T_q^{''} \cdot s}{1 + T_{q0}^{''} \cdot s} \cdot x_q$$

The transient and sub-transient time constants are well known from machine theory. The assumptions usually made are:

$$T_1 + T_2 = T_{d0}^{'} + T_{d0}^{''} \qquad T_1 \cdot T_3 = T_{d0}^{'} \cdot T_{d0}^{''}$$

$$T_4 + T_5 = T_d^{'} + T_d^{''} \qquad T_4 \cdot T_6 = T_d^{'} \cdot T_d^{''}$$

These time constants can be expressed as:

$$T_1 = \frac{x_{md} + x_{f\sigma}}{\omega_n \cdot r_f} = \frac{x_f}{\omega_n \cdot r_f} = T_f \approx T_{d0}^{'} \qquad T_2 = \frac{x_{md} + x_{D\sigma}}{\omega_n \cdot r_D} = \frac{x_D}{\omega_n \cdot r_D} = T_D$$

$$T_3 = \frac{1}{\omega_n \cdot r_D} \left[x_{D\sigma} + \frac{1}{\frac{1}{x_{md}} + \frac{1}{x_{f\sigma}}} \right] \approx T_{d0}^{''} \qquad T_4 = \frac{1}{\omega_n \cdot r_f} \left[x_{f\sigma} + \frac{1}{\frac{1}{x_{md}} + \frac{1}{x_{s\sigma}}} \right] \approx T_d^{'}$$

$$T_5 = \frac{1}{\omega_n \cdot r_D} \left[x_{D\sigma} + \frac{1}{\frac{1}{x_{md}} + \frac{1}{x_{s\sigma}}} \right] \qquad T_6 = \frac{1}{\omega_n \cdot r_D} \left[x_{D\sigma} + \frac{1}{\frac{1}{x_{md}} + \frac{1}{x_{s\sigma}} + \frac{1}{x_{f\sigma}}} \right] \approx T_d^{''}$$

$$T_{D\sigma} = \frac{x_{D\sigma}}{\omega_n \cdot r_D}$$

$$T''_{q0} = \frac{x_{mq} + x_{Q\sigma}}{\omega_n \cdot r_Q} = \frac{x_Q}{\omega_n \cdot r_Q} = T_Q \qquad T''_q = \frac{1}{\omega_n \cdot r_Q}\left[x_{Q\sigma} + \frac{1}{\frac{1}{x_{mq}} + \frac{1}{x_{s\sigma}}} \right]$$

The equivalent scheme is shown in Figure 3.8. This model will be discussed more in details when analysing the current controllers. The field current can be expressed as:

$$i_f(s) = G(s) \cdot \frac{1 + T_D \cdot s}{1 + T_{D\sigma} \cdot s} \cdot \frac{1}{x_{md}} \cdot u_f(s) - s \cdot G(s) \cdot i_d(s)$$

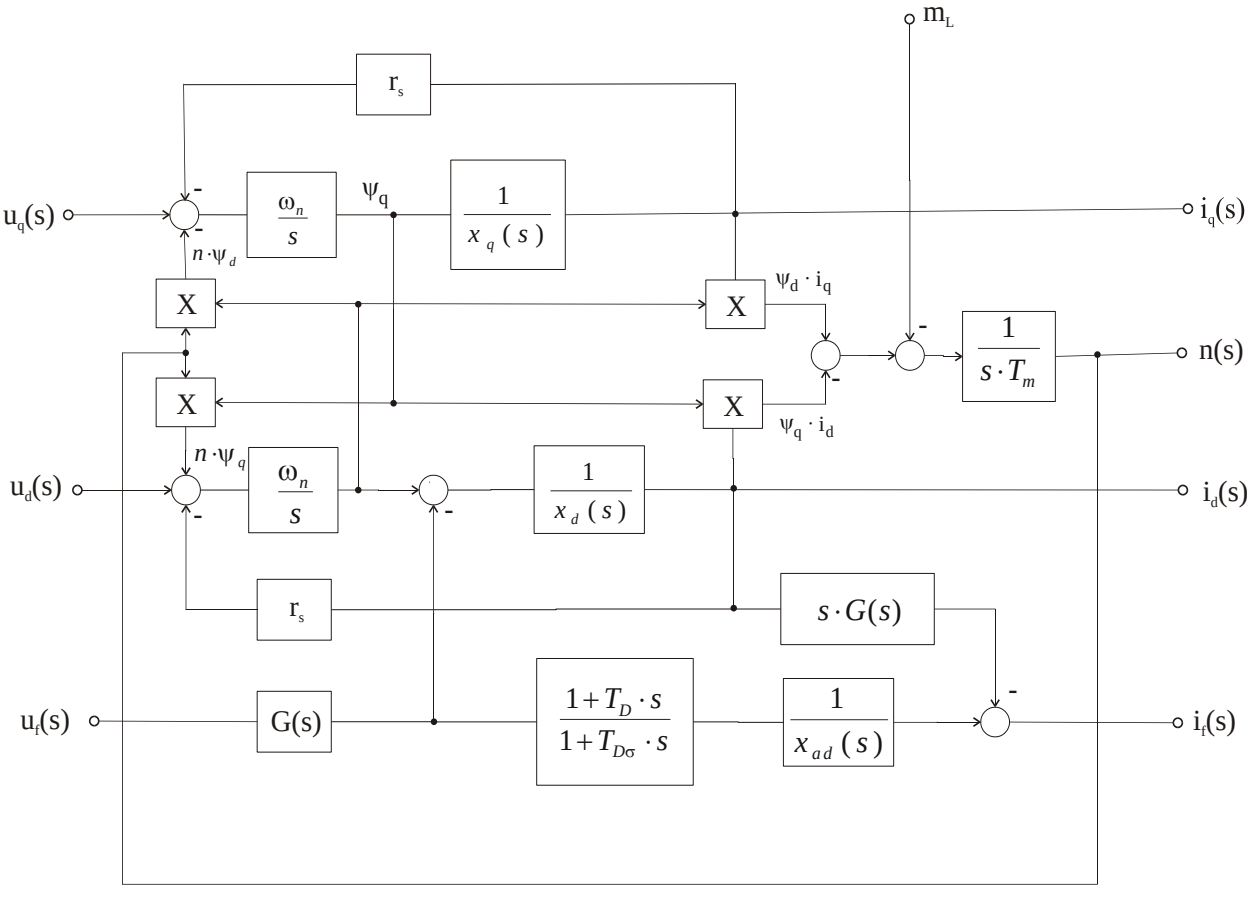

Figure 3.8: Equivalent scheme for a 3-phase Synchronous Machine

3.4 Motor Control

The control strategy chosen for the torque control is the unity power factor control, i.e. cosφ=1 control. When neglecting the ohmic stator losses, this means to locate the stator current space vector perpendicular to the space vector of the stator flux:

$$\tau_e = \underline{\psi}_s \otimes \underline{i}_s = \psi_s \cdot i_s$$

The amplitude of the stator flux vector is in steady state kept constant by help of the field current i_f . The space vector diagram for unity power factor control is shown in Figure 3.9. The current references can be calculated based on the torque reference and stator flux reference as follows:

$$\tan\delta_{ref} = \pm\frac{x_q i_{sref}}{\psi_{sref}} = \frac{x_q \tau_{eref}}{\psi_{sref}^2} \qquad i_{sref} = \frac{|\tau_{eref}|}{\psi_{sref}} \qquad i_{dref} = -i_{sref}\cdot\sin\delta_{ref} \qquad i_{qref} = i_{sref}\cdot\cos\delta_{ref}$$

To keep the stator flux equal the required reference value, the steady state value of the field current should be equal:

$$i_{fref} = \frac{1}{x_{md}}\frac{\psi_{sref}^2 + x_d x_q i_{sref}^2}{\sqrt{\psi_{sref}^2 + x_q^2 i_{sref}^2}}$$

These formulas for calculation of reference values are valid for steady state conditions. If improved dynamic response is required, some modifications could be introduced. One option is to introduce a stator flux amplitude controller giving the field current reference as output. This will, however, only directly influence the d-axis flux as shown in the previous sub-section.

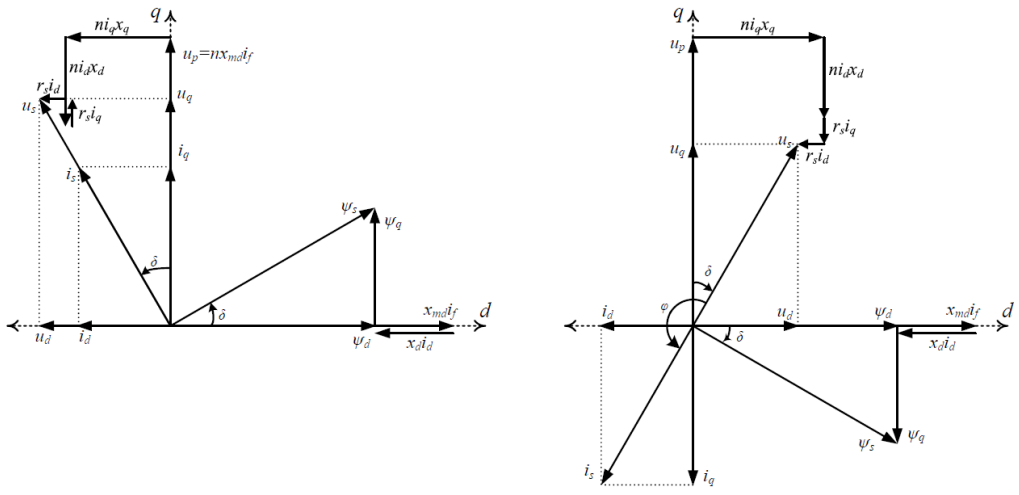

Figure 3.9: Space vector diagram for Synchronous Machine in motor- and generator mode (n>0)

3..4.1 Stator current controllers

The classical way to tune the PI current controllers in the dq-frame is to use decoupling terms and Modulus Optimum. The time delay in the inverter, the filter time constant and time delay in the processor are lumped into a time constant of a 1st order filter with time constant T_{sum} (u_{dc}=1):

$$h_{oid} = K_{pd}\frac{1+T_{i,d}\cdot s}{T_{i,d}\cdot s}\frac{1}{r_d^{''}\cdot\left(1+T_d^{''''}\cdot s\right)\cdot\left(1+T_{sum}\cdot s\right)} \qquad T_d^{''''} = \frac{x_d^{''}}{\omega_n\cdot r_d^{''}} \qquad \mathrm{T_{sum}} = T_{delay}+T_{fd}$$

$$h_{oiq} = K_{pq}\frac{1+T_{i,q}\cdot s}{T_{i,q}\cdot s}\frac{1}{r_q^{''}\cdot\left(1+T_q^{''''}\cdot s\right)\cdot\left(1+T_{sum}\cdot s\right)} \qquad T_q^{''''} = \frac{x_q^{''}}{\omega_n\cdot r_q^{''}} \qquad \mathrm{T_{fd}} = T_{fq}$$

The decoupling terms can be chosen as:

$$u_{dII} = -\frac{r_{Rd}^{'}}{x_{Md}}\cdot\psi_{Rd} + r_{Rd}^{'}\cdot i_f + k_{fD}\cdot\left(u_f - r_f\cdot i_f\right) - n\cdot\psi_q$$

$$u_{qII} = -\frac{r_{Rq}}{x_{Mq}}\cdot\psi_{Rq} + n\cdot\psi_d$$

This will require estimated values of the flux linkages in the d- and q-axis damper windings. This is the method chosen, but without decoupling terms. For a digital controller with asymmetrical modulation (T_{samp}= T_{tri}/2 and T_{tri} =1/f_{sw}) and a moving average filter, one obtains:

$$K_{pd} = \frac{T_d^{''''} - \frac{T_{samp}}{2}}{2\cdot\frac{1}{r_d^{''}}\cdot\left(T_{sum}+\frac{T_{samp}}{2}\right)} \approx \frac{x_d^{''}}{2\cdot\omega_n\cdot\left(\frac{5}{4}\cdot T_{tri}\right)} = \frac{x_d^{''}}{5\cdot\omega_n\cdot T_{samp}} \qquad \mathrm{T_{i,d}} = \frac{x_d^{''}}{\omega_n\cdot r_d^{''}}$$

$$K_{pq} = \frac{x_q^{''}}{\frac{5}{2}\cdot\omega_n\cdot T_{tri}} = \frac{x_q^{''}}{5\cdot\omega_n\cdot T_{samp}} \qquad \mathrm{T_{i,q}} = \frac{x_q^{''}}{\omega_n\cdot r_q^{''}}$$

Another approach can be based on the transfer-functions $x_d(s)$ and $x_q(s)$. The stator voltage equations can then be expressed as [4]:

$$u_d(s) = r_s\cdot\left(1+\frac{s\cdot x_d(s)}{\omega_n\cdot r_s}\right)\cdot i_d(s) - \frac{s}{\omega_n}\cdot G(s)\cdot u_f(s) - n\cdot\psi_q(s)$$

$$u_q(s) = r_s\cdot\left(1+\frac{s\cdot x_q(s)}{\omega_n\cdot r_s}\right)\cdot i_q(s) + n\cdot\psi_d(s)$$

The cross-over frequency of the current control loop will be at high frequencies. This means that around these frequencies the equations can be simplified to (n=0 and u_f constant) :

$$u_d(s) \approx r_s \cdot \left(1 + \frac{s \cdot x_d''}{\omega_n \cdot r_s}\right) \cdot i_d(s) \approx \frac{s \cdot x_d''}{\omega_n} \cdot i_d(s) \qquad T_{d0}' \approx \frac{x_d}{x_d'} \cdot T_d' \qquad T_{d0}'' \approx \frac{x_d'}{x_d''} \cdot T_d''$$

$$u_q(s) \approx r_s \cdot \left(1 + \frac{s \cdot x_q''}{\omega_n \cdot r_s}\right) \cdot i_q(s) \approx \frac{s \cdot x_q''}{\omega_n} \cdot i_q(s) \qquad T_{q0}'' = \frac{x_q}{x_q''} \cdot T_q''$$

If the first assumption is used, Modulus Optimum can be applied:

$$h_{oid} = K_{pd} \frac{1 + T_{i,d} \cdot s}{T_{i,d} \cdot s} \cdot \frac{1}{r_s \cdot \left(1 + \frac{s \cdot x_d''}{\omega_n \cdot r_s}\right) \cdot (1 + T_{sum} \cdot s)} \qquad \mathrm{T_{sum}} = T_{delay} + T_{fd}$$

$$h_{oiq} = K_{pq} \frac{1 + T_{i,q} \cdot s}{T_{i,q} \cdot s} \cdot \frac{1}{r_s \cdot \left(1 + \frac{s \cdot x_q''}{\omega_n \cdot r_s}\right) \cdot (1 + T_{sum} \cdot s)} \qquad \mathrm{T_{fd}} = T_{fq}$$

The gain and integral time constants of the PI current controllers then become:

$$K_{pd} = \frac{\frac{x_d''}{\omega_n \cdot r_s} - \frac{T_{samp}}{2}}{2 \cdot \frac{1}{r_s} \cdot \left(T_{sum} + \frac{T_{samp}}{2}\right)} \approx \frac{x_d''}{2 \cdot \omega_n \cdot \left(\frac{5}{4} \cdot T_{tri}\right)} = \frac{x_d''}{5 \cdot \omega_n \cdot T_{samp}} \qquad \mathrm{T_{i,d}} = \frac{x_d''}{\omega_n \cdot r_s}$$

$$K_{pq} = \frac{x_q''}{\frac{5}{2} \cdot \omega_n \cdot T_{tri}} = \frac{x_q''}{5 \cdot \omega_n \cdot T_{samp}} \qquad \mathrm{T_{i,q}} = \frac{x_q''}{\omega_n \cdot r_s}$$

If the second assumption is chosen, Symmetrical Optimum can be used:

$$h_{oid} = K_{pd} \frac{1 + T_{i,d} \cdot s}{T_{i,d} \cdot s} \cdot \frac{\omega_n}{s \cdot x_d'' \cdot (1 + T_{sum} \cdot s)} \qquad \mathrm{T_{sum}} = T_{delay} + T_{fd}$$

$$h_{oiq} = K_{pq} \frac{1 + T_{i,q} \cdot s}{T_{i,q} \cdot s} \cdot \frac{\omega_n}{s \cdot x_q'' \cdot (1 + T_{sum} \cdot s)} \qquad \mathrm{T_{fd}} = T_{fq}$$

The calculation of the control parameters then becomes:

$$K_p = \frac{x_d''}{\sqrt{\beta} \cdot \omega_n \cdot (T_{sum} + \frac{T_{samp}}{2})} \qquad T_i = \beta \cdot \left(T_{sum} + \frac{T_{samp}}{2}\right) \qquad \omega_c \approx \nu_c = \frac{1}{\sqrt{\beta} \cdot \left(T_{sum} + \frac{T_{samp}}{2}\right)}$$

When taking into account time delays and filter, this gives:

$$K_{pd} = \frac{x_d^{"}}{\sqrt{\beta}\cdot\omega_n\cdot\left(\frac{5}{4}\cdot T_{tri}\right)} \qquad K_{pq} = \frac{x_q^{"}}{\sqrt{\beta}\cdot\omega_n\cdot\left(\frac{5}{4}\cdot T_{tri}\right)} \qquad T_{i,d} = T_{i,q} = \beta\cdot\left(\frac{5}{4}\cdot T_{tri}\right)$$

If β is chosen equal 4, the gains will be similar to the gains for Modulus Optimum. However, the integral time constants will be different and the overshoot will be 40 %. This is not optimal for current controllers, while this may trip the drive due to over-currents. A value of β between 6 and 10 can be tested. The phase margin at the crossover frequency will then be larger than needed, such that the gains can be increased compared to the gains given by the formulas. This will improve the response of the controllers.

3.4.2 Field Current Controller

The field current PI controller can be designed in the dq-frame by using a decoupling term and Modulus Optimum. The time delay in the inverter, the filter time constant and time delay in the processor are lumped into a time constant of a 1st order filter ($u_{dc,f}$=1):

$$h_{oif} = K_{pf}\frac{1+T_{i,f}\cdot s}{T_{i,f}\cdot s}\frac{1}{r_f^{"}\cdot\left(1+T_f^{"}\cdot s\right)\cdot\left(1+T_{sum}\cdot s\right)} \qquad T_f^{"} = \frac{x_f^{"}}{\omega_n\cdot r_f^{"}} \qquad \mathrm{T_{sum}} = T_{delay} + T_{ff}$$

The decoupling terms can be chosen as:

$$u_{fII} = -\frac{r_{Rd}^{"}}{x_{Md}}\cdot\psi_{Rd} + r_{Rd}^{"}\cdot i_d + k_{dD}\cdot\left(u_d - r_s\cdot i_d + n\cdot\psi_q\right)$$

This gives:

$$K_{pf} = \frac{\frac{x_f^{"}}{\omega_n\cdot r_f^{"}} - \frac{T_{samp}}{2}}{2\cdot\frac{1}{r_f^{"}}\cdot\left(T_{sum}+\frac{T_{samp}}{2}\right)} \approx \frac{x_f^{"}}{2\cdot\omega_n\cdot\left(\frac{5}{4}\cdot T_{tri}\right)} = \frac{x_f^{"}}{5\cdot\omega_n\cdot T_{samp}} \qquad \mathrm{T_{i,f}} = T_f^{"} = \frac{x_f^{"}}{\omega_n\cdot r_f^{"}}$$

As for the stator currents a transfer-function approach can be used. This field current can then be expressed as:

$$i_f(s) = G(s)\cdot\frac{1+T_D\cdot s}{1+T_{D\sigma}\cdot s}\cdot\frac{1}{x_{md}}\cdot u_f(s) - s\cdot G(s)\cdot i_d(s)$$

A simplified expression becomes:

$$i_f(s) \approx \frac{1+T_D \cdot s}{(1+T_{d0}^{'} \cdot s)\cdot(1+T_{d0}^{''} \cdot s)} \cdot \frac{u_f(\mathrm{s})}{r_f} - \frac{\mathrm{s}\cdot(1+T_{D\sigma} \cdot s)}{(1+T_{d0}^{'} \cdot s)\cdot(1+T_{d0}^{''} \cdot s)} \cdot \frac{x_{md}}{r_f} \cdot i_d(s)$$

If we assume i_d constant, Modulus Optimum can be used:

$$h_{oif} = K_{pf} \frac{1+T_{i,f} \cdot s}{T_{i,f} \cdot s} \cdot \frac{1+T_D \cdot s}{r_f \cdot (1+T_{d0}^{'} \cdot s)\cdot(1+T_{d0}^{''} \cdot s)\cdot(1+T_{sum} \cdot s)} \qquad \mathrm{T_{sum}} = T_{delay} + T_{ff}$$

The most classical approximation used is:

$$h_{oif} = K_{pf} \frac{1+T_{i,f} \cdot s}{T_{i,f} \cdot s} \cdot \frac{1}{r_f \cdot (1+T_{d0}^{'} \cdot s)\cdot(1+T_{sum} \cdot s)} \qquad \mathrm{T_{sum}} = T_{delay} + T_{ff}$$

A more detailed analysis is performed in [4]. Modulus Optimum then gives:

$$K_{pf} = \frac{\frac{x_f}{\omega_n \cdot r_f} - \frac{T_{samp}}{2}}{2 \cdot \frac{1}{r_f} \cdot \left(T_{sum} + \frac{T_{samp}}{2}\right)} \approx \frac{x_f}{2 \cdot \omega_n \cdot \left(\frac{5}{4} \cdot T_{tri}\right)} = \frac{x_f}{5 \cdot \omega_n \cdot T_{samp}} \qquad \mathrm{T_{i,f}} = T_{d0}^{'} = T_f = \frac{x_f}{\omega_n \cdot r_f}$$

In practice, this gain becomes too high due to amplification of the current ripple. Another option is to increase the filtering and thus reduce the gain.

3.4.3 Stator Flux Amplitude Controller

To improve the control of the stator flux amplitude a closed loop control can be implemented. The calculated field current reference given by the formula presented above can be used as a feedforward term. To implement such a controller an estimated value of the flux amplitude has to be provided. One option is to use the classical voltage model combined with a current model for low speed operation. Here we will assume that the flux can be measured and focus on the design of the controller.

The approach is to use i_f for controlling the stator flux amplitude. This current, however, is mainly controlling the d-component of the stator flux only. This design of the controller can be based on the following equations:

$$\psi_d = \psi_{Rd} + \sigma_{dD} \cdot x_d \cdot i_d + \sigma_D \cdot x_{Md} \cdot i_f$$

$$T_D \cdot \frac{d\psi_{Rd}}{dt} = -\psi_{Rd} + x_{Md} \cdot (i_d + i_f)$$

If modelling the closed response of the field current control loop as a 1st order transfer-function with the time constant $T_{eq,f}$, one obtains:

$$h_{oi\psi} = K_{p\psi}\frac{1+T_{i,\psi}\cdot s}{T_{i,\psi}\cdot s}\cdot\frac{x_{Md}}{(1+T_D\cdot s)\cdot(1+T_{sum}\cdot s)} \qquad \mathrm{T_{sum}} = T_{eq,f} + T_{ff} = 2\cdot T_{sum,f} + T_{ff}$$

Use of Modulus Optimum gives:

$$K_{p\psi} = \frac{\frac{x_{Md}}{\omega_n\cdot r_{Rd}} - \frac{T_{samp}}{2}}{2\cdot x_{Md}\cdot\left(T_{sum}+\frac{T_{samp}}{2}\right)} \approx \frac{1}{2\cdot r_{Rd}\cdot\omega_n\cdot\left(T_{sum}+\frac{T_{tri}}{4}\right)} \qquad \mathrm{T_{i,\psi}} = T_D = \frac{x_{Md}}{\omega_n\cdot r_{Rd}}$$

It is important to investigate the influence of the q-component of the stator flux. In addition, the filtering of the flux amplitude will influence the bandwidth of the controller.

Because a flux model is not implemented in the controller for the time being, and some time delays in the communications between controllers in the 100 kW set-up, this controller concept will not be further investigated in this report. Some investigations have been executed in a specialization project at NTNU in 2017.

3.5 Test results

In this section tuning of current controllers as well the torque control response is tested by help of the Emulator in the FPGA.

3.5.1 Current controllers

When testing the controllers in the d-axis, i.e. d-axis stator current controller and the field current controller, it is important to be aware about the coupling between these controllers. When both controllers are tuned to have fast response, this becomes important.

Stator d-axis current controller is tested with a step in the reference value at zero speed. Two different tests are performed:

- With constant reference voltage equal 0 for the field converter
- With the field current controller enabled and a field current reference equal 0

In the first case the equivalent stator current controller will observe the sub-transient inductance, while in the second case a bit increase in the equivalent inductance can be assumed. The current response is however quite similar. The reason for this is that the field current controller is a bit slower than the d-axis stator current controller, which means that the circuit looks quite similar as in the first case.

The step is restricted to 0.1 pu to avoid that the controller is limited. This is required to be able to observe the effect of parameter tuning.

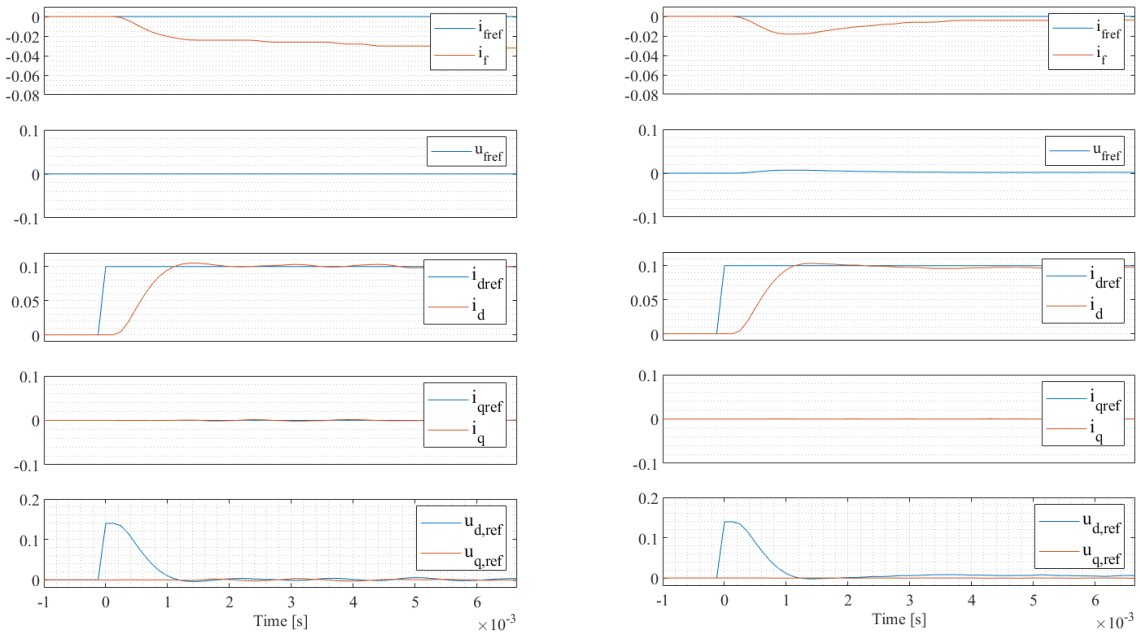

a) Field Controller Disabled *b) Field Controller Enabled*

Figure 3.10: Step response of the d-axis stator current controller 0 to 0.1 pu (n=0)

Similar tests were made when tuning the field current controller. In this case it was the stator controller, which was disabled and enabled:

- With constant reference voltage equal 0 for the stator inverter
- With the stator current controllers enabled and current references equal 0

Both the d- and q-axis stator current controllers were operated in the same way. When investigating the tuning of the field current controller, only a small step of 0.02 pu in the reference value is applied, to avoid that the PI controller is in limitation. The behavior is according to symmetrical optimum.

When investigating the effect of enabling the stator current controller, i.e. the coupling between the controllers especially in the d-axis, a step in the field current reference of 1 pu is applied. It can then be seen that, due to the fast stator current controller, the d-axis current can be interpreted almost as a current source. This means that the parallel path of damper winding and stator winding is not present. This means that the time constant observed by the field winding becomes somewhat larger. The result is a bit slower for the field current response when the controller is in saturation as shown when comparing Figure 3.11b and Figure 3.12.

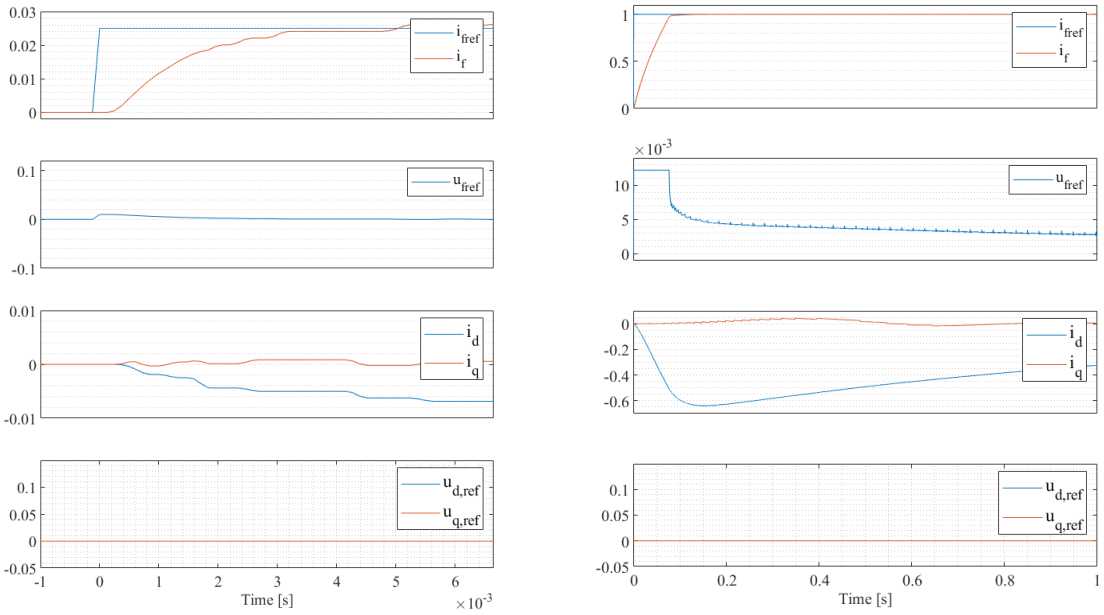

a) Step in i_{fref} from 0 to 0.02 pu *b) Step in i_{fref} from 0 to 1.0 pu*

Figure 3.11: Step response of the field current controller when stator current controllers are disabled (n=0)

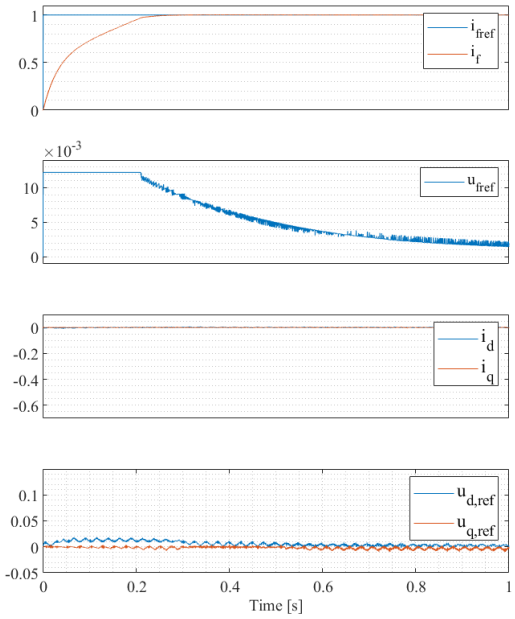

Figure 3.12: Step response of the field current controller from 0 to 1 pu with stator current controllers enabled (n=0)

3.5.2 Torque Control

The strategy chosen for torque control is as mentioned earlier the Unity Power Factor Control. The amplitude of the stator flux vector is in steady state kept constant by help of the field current i_f . The space vector diagram for unity power factor control is shown in Figure 3.9. The current references can be calculated based on the torque reference and stator flux reference as follows:

$$\tan\delta_{ref} = \pm\frac{x_q i_{sref}}{\psi_{sref}} = \frac{x_q \tau_{eref}}{\psi_{sref}^2} \qquad i_{sref} = \frac{|\tau_{eref}|}{\psi_{sref}} \qquad i_{dref} = -i_{sref}\cdot\sin\delta_{ref} \qquad i_{qref} = i_{sref}\cdot\cos\delta_{ref}$$

This means that for increased torque a more negative stator d-axis current is required. In addition, an increase q-axis current is required as well. To keep the stator flux equal the required reference value, the steady state value of the field current should be increased for compensating the negative d-axis stator current:

$$i_{fref} = \frac{1}{x_{md}}\frac{\psi_{sref}^2 + x_d x_q i_{sref}^2}{\sqrt{\psi_{sref}^2 + x_q^2 i_{sref}^2}}$$

The change in d-axis damper winding flux linkages is thus usually less than the change in q-axis damper winding flux linkages:

$$T_D\cdot\frac{d\psi_{Rd}}{dt} = -\psi_{Rd} + x_{Md}\cdot\left(i_d + i_f\right)$$

$$T_Q\cdot\frac{d\psi_{Rq}}{dt} = -\psi_{Rq} + x_{Mq}\cdot i_q$$

From the torque equation one can see that a sudden step in i_q gives a sudden step in torque, however, a further increase in torque will occur due to the time constant T_Q . This happens if i_d is different from zero due to the term ψ_{Rq}*i_d. The value of ψ_{Rd} usually do not change that much due to compensation of armature reaction with i_f

$$\tau_e = \psi_d\cdot i_q - \psi_q\cdot i_d = \psi_{Rd}\cdot i_q - \psi_{Rq}\cdot i_d + \left(\sigma_D\cdot x_{Md}\cdot i_f + \left(\sigma_{dD}\cdot x_d - \sigma_{qQ}\cdot x_q\right)\cdot i_d\right)\cdot i_q$$

In Figure 3.13 a step response in the torque reference from the PLC from 0 to 0.9 pu is shown. It is clear that an instant step due to the step in i_q occur very fast. However, an addition increase in the torque due to the 1st order response of the q-axis damper winding can be observer.

The ψ_{Rd} is somewhat reduce for increased loading to keep the requreid amplitude for of ψ_s while ψ_{Rq} increases with increased load.

The time response of torque is acceptable for this type of load. Some dynamical boosting of i_q can be introduced if required.

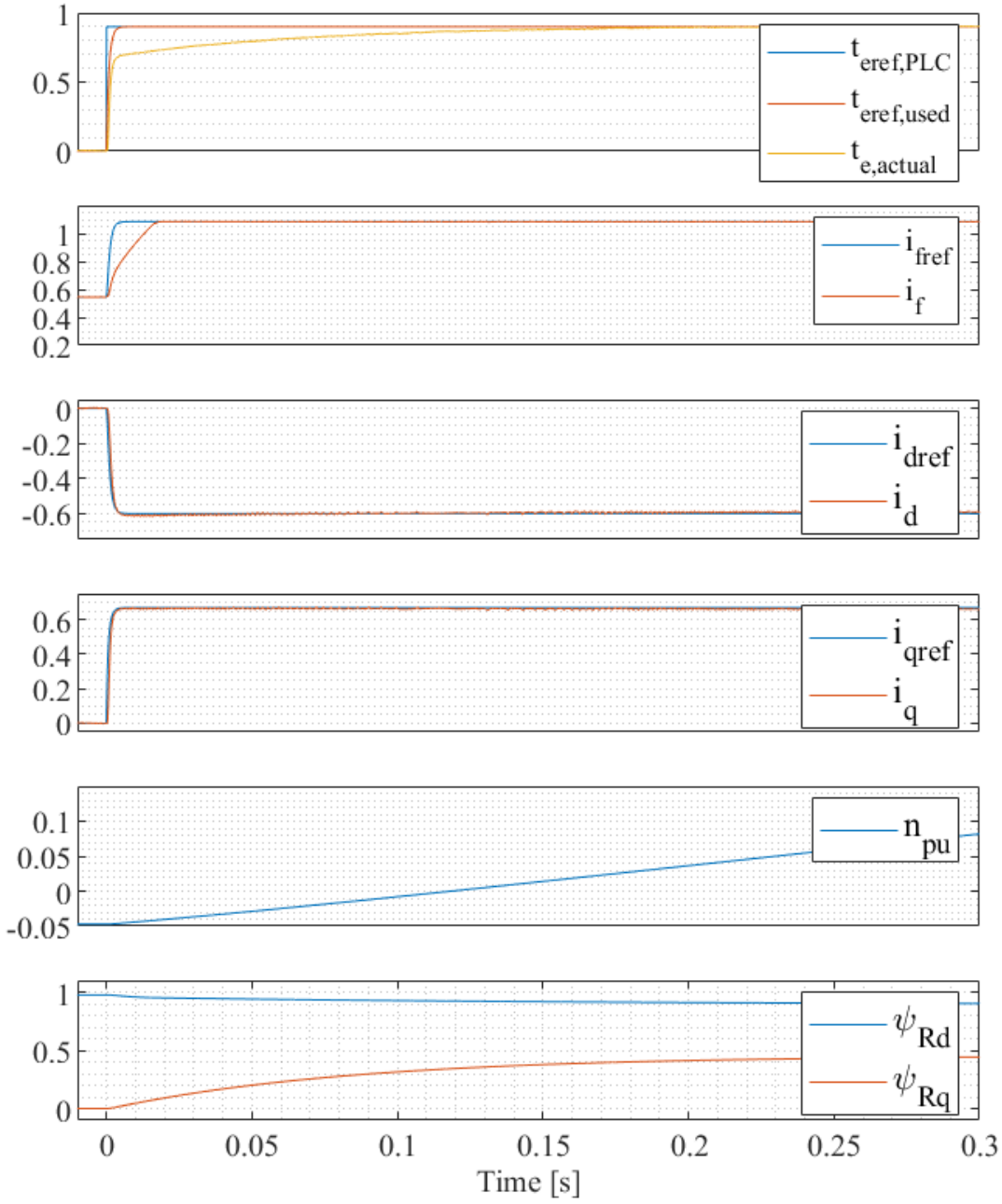

Figure 3.13: Step in PLC torque reference from 0 to 0.9 pu. A 1ms 1st order low pass filtering of torque ref.

4 A 100 kW Synchronous Motor Drive

In this chapter a system description is provided. In addition, the results of tuning of the controllers are presented. The controllers are stator d-a and q-axis, current controllers, field current controllers, speed controller and DC-link voltage controller.

4.1. System descriptions

An overview of the complete set-up is shown in Figure 4.1. It consists of two motor drive; an Induction Motor Drive and a Synchronous Motor Drive. In this chapter the SM drive is in focus.

The SM Drive consists of a full-bridge field exciter converter and a 3-phase 2-level stator inverter. The SM control is implemented in 2 different control boards; one for the filed exciter and one for the motor control. The motor control board is the master and the field exciter control board is the slave. The communication between the boards is implemented with a CAN-bus, which gives a delay/update-rate of typical 300 ms. The signals transferred between the control boards are listed in Figure 4.2. The ideal case would have been that the exciter converter was also controlled from the same control board which is used for control of SM converter. But the exciter converter already exists for a conventional operation of synchronous machine in a direct grid connected mode. Therefore, CAN bus communication was established to control the exciter converter based on unity power factor strategy implemented in the SM converter.

The SM control mode used are speed control and DC-link voltage control. In the SM control some torque limiter functions are implemented. Especially the DC-link under- and over-voltage limiter will be in action during the Low Voltage Ride Through tests presented in the next chapter. This function is important when the motor drive is not in DC-link voltage control mode.

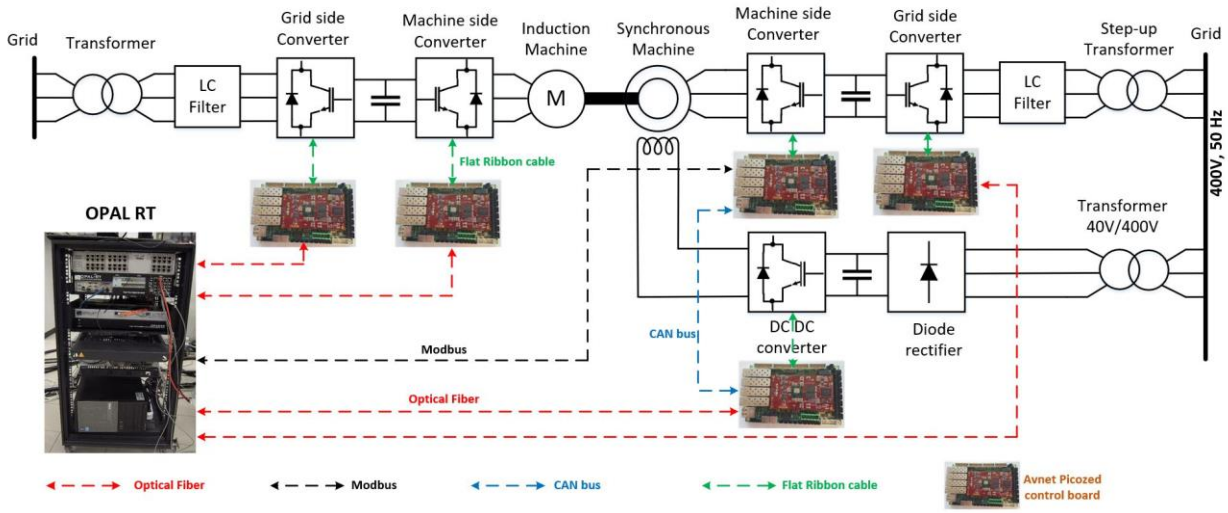

Figure 4.1: The 100 kVA Drive Set Up

Signals	Description
SM converter → Exciter converter	
Power On	Turns on the breaker and dc-link of the exciter converter is powered on
Gate driver On	Switching pulses to the dc-dc converter is enabled
Exciter current reference	Current reference is set to the exciter based on unity power factor strategy implemented in the SM converter

Exciter converter → SM converter	
Power On status	Status to show that dc-link is powered on
Gate driver on status	Status to show that gate pulses are enabled
Exciter current actual	Measured current from the exciter

Figure 4.2: Signals transferred between Motor Control Board and Field Exciter Control Board

The Active Front End (AFE) converter have two control modes; DC-link voltage control mode and PQ-control mode. The first mode is used when the system is in pump mode, while the second one when the system is in turbine mode. The change of mode is controlled by the Opal RT.

4.2. Current Controllers

The Synchronous Motor used is a custom designed machine for NTNU purchased from BEVI. The data in the test report is somewhat limited, but sufficient for design of some of the controller. The rated data is presented in Figure 4.3. In addition to these data, some test results for sub-transient parameters were also provided. These parameters are:

$$x_d^{''} = 0.3359\ [pu] \qquad r_d^{''} = 0.2325\ [pu] \qquad x_q^{''} = 0.3176\ [pu] \qquad r_q^{''} = 0.2369\ [pu]$$

The test conditions used during test is not quite clear. Some dependency of currents, flux level, temperature and frequency will influence the test results. However, the given parameter values will be used for calculation of the initial value for the controller parameters in the stator current controllers.

Synchronous Machine Specification	
Rated Power	100 kVA
Rated voltage	400 V
Rated current	144.3 A
Rated speed	428.57 rpm
x_d	1.27 pu
x_q	0.75 pu
Rated field current (I_f)	56 A

Figure 4.3: Rated data of the 100 kVA Synchronous Machine

4.2.1 Stator current controllers

The parameters of the PI controllers are calculated based on the Modulus Optimum criterion presented earlier in this report. The sampling frequency of the controller is 8 kHz, i.e. T_{samp} is equal 125 µs. The rated frequency of the machine is 50 Hz. This gives:

$$K_{pd} = \frac{x_d''}{5 \cdot \omega_n \cdot T_{samp}} = 1.71 \ [pu] \quad T_{i,d} = \frac{x_d''}{\omega_n \cdot r_d''} = 0.0046 \ [s]$$

$$K_{pq} = \frac{x_q''}{5 \cdot \omega_n \cdot T_{samp}} = 1.61 \ [pu] \quad T_{i,q} = \frac{x_q''}{\omega_n \cdot r_q''} = 0.0042 \ [s]$$

When tuning the controllers in the lab, different approaches can be chosen. The step response of the d-axis current controller can be made with or without the field current controller activated. As shown in the previous chapter, the response of the d-axis current controller does not differ very much. In this case the field current controller was activated with 20 A field current reference. The tuning was executed before calculating the theoretical values presented above, but one can see that the gains are very similar. The integral time constant was chosen a bit smaller in the lab, which gave a bit more overshoot than according to Modulus Optimum. The current rise time is typical 4-5 T_{samp} , i.e. typical 0.7 ms as shown in Figure 4.4. This is somewhat faster than for the case of Modulus Optimum.

When tuning the q-axis current controller, the refence value is toggled between +/- 0.1 pu to avoid acceleration of the machine. The q-axis controller is also tuned to have more overshoot and faster response than when using the Modulus Optimum Criterion.

It is interesting to observe that parameters obtained from the test results in the factory give acceptable results in the lab, even though a bit more aggressive tuning of the integral time constants has been chosen in the final set-up.

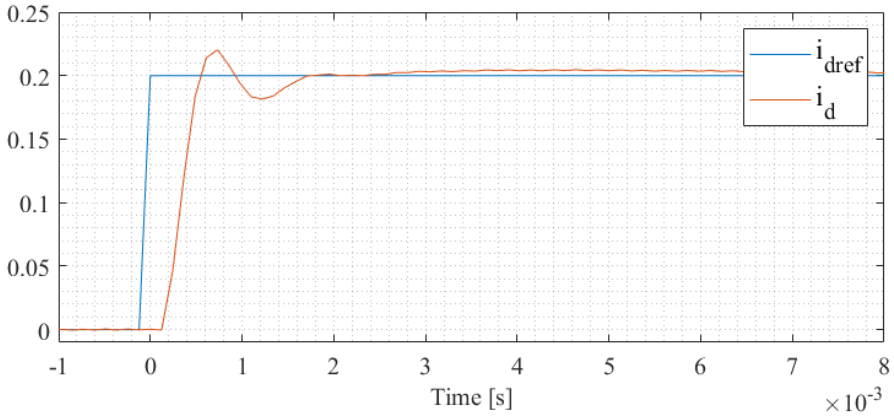

Figure 4.4: Step response of the d-axis stator current controller: K_{pd}= 1.75 and $T_{i,d}$=2.5 ms

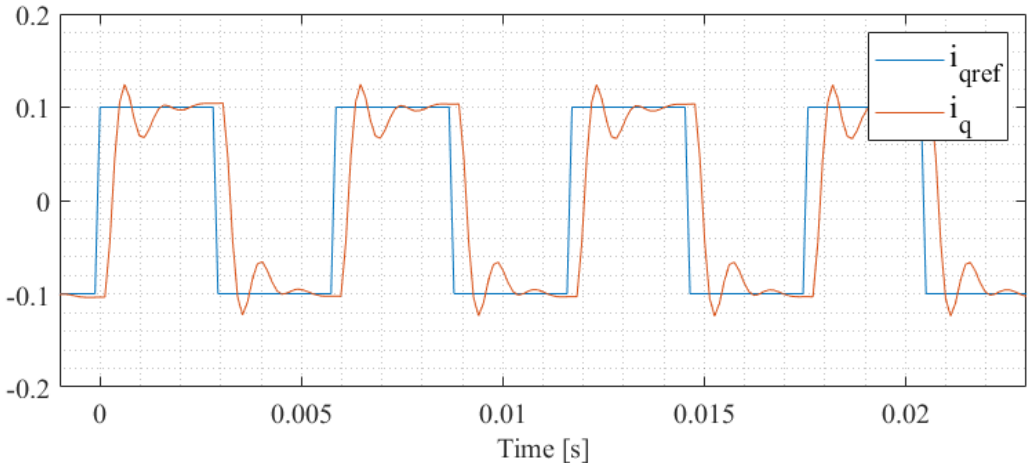

Figure 4.5: Step response of the q-axis stator current controller: K_{pq}= 2.2 and $T_{i,q}$=1.5 ms

4.2.2 Field current controller

The field current controller is tuned by SINTEF. The design rule used has been Symmetrical Optimum with β=10. The filter used for filtering the measured current is 2 ms. The controller parameters are:

$$K_{pf}=1.5\ [pu] \quad T_{i,f}=0.2\ [s] \qquad T_{f,filter}=2\ [ms]$$

4.3. Motor Control Modes

The control modes used in this project are speed control and dc-link voltage control. Other control modes as torque control and power control are possible as well.

Due to the control modes to be used, a speed controller and a dc-link voltage controller has to be designed. The output of these controllers is the torque reference.

4.3.1 Speed Controller

Choice of the speed controller is very dependent on the actual application. The inner torque control loop can usually be represented as a 1st order transfer function when designing the speed controller. A simplified model of the speed control loop is then:

$$h_{o,n}(s)=\frac{1}{T_m\cdot s}\cdot\frac{\psi_{af}}{(1+T_{eq,i}\cdot s)\cdot(1+T_{f,n}\cdot s)}\cdot\frac{\tau_{eref}}{\psi_{afref}(i_{fref})}$$
$$=\frac{1}{T_m\cdot s}\cdot\frac{\tau_{eref}}{(1+T_{eq,i}\cdot s)\cdot(1+T_{f,n}\cdot s)}$$

The total open loop transfer function with a PI-controller can then be expressed as:

$$h_{o,n}(s) = \frac{1}{T_m \cdot s} \cdot \frac{1}{(1 + T_{eq,i} \cdot s) \cdot (1 + T_{f,n} \cdot s)} \cdot K_{pn} \cdot \frac{1 + T_{in} \cdot s}{T_{in} \cdot s}$$

$$h_{o,n}(s) = \frac{1}{T_m \cdot s} \cdot \frac{1}{(1 + T_{sum,n} \cdot s)} \cdot K_{pn} \cdot \frac{1 + T_{in} \cdot s}{T_{in} \cdot s} \qquad T_{sum,n} = T_{eq,i} + T_{f,n}$$

Use of Symmetrical Optimum gives:

$$K_{pn} = \frac{T_m}{\sqrt{\beta} \cdot T_{sum,n}} \qquad T_{in} = \beta \cdot T_{sum,n} \qquad \omega_{cn} = \frac{1}{\sqrt{\beta} \cdot T_{sum,n}}$$

The equivalent time constant $T_{eq,I}$ of the torque control loop is less than 1 ms. However, taken into account that also the field current control is involved in the torque control, an equivalent time constant $T_{sum,n}$ equal 40 ms is used. With T_m=2 H= 2.5 sec and β=10, the parameters become:

$$K_{pn} = \frac{T_m}{\sqrt{\beta} \cdot T_{sum,n}} = 20.0 \qquad T_{in} = \beta \cdot T_{sum,n} = 0.4\ [s]$$

The speed reference is filtered by a first order low pass filter with time constant (T_f) = 100 ms. The step-response is shown in Figure 4.6

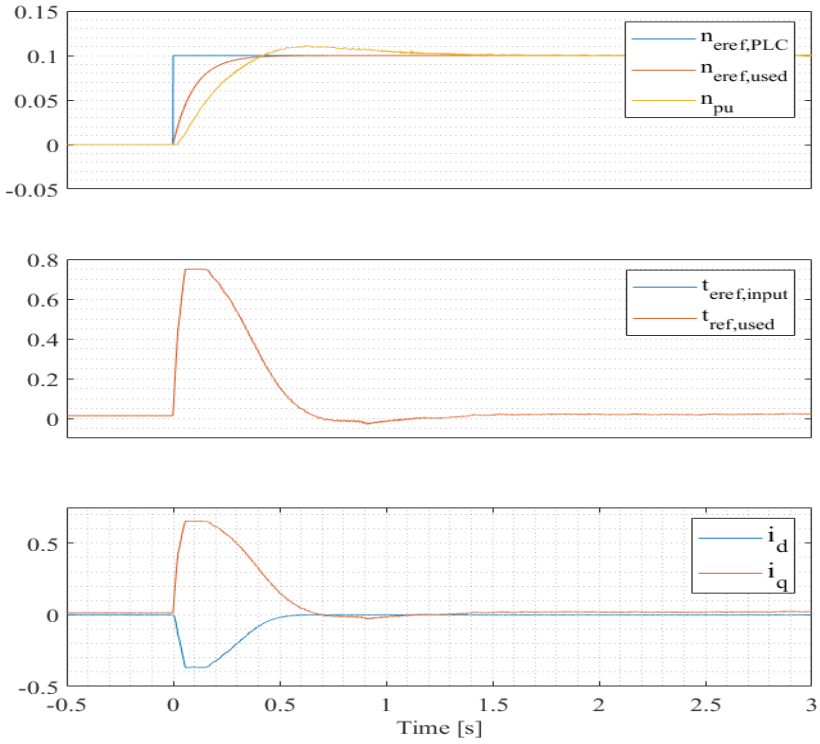

Figure 4.6: Step response of the speed controller: K_{pn}= 10.0 and $T_{i,n}$=0.4 s

4.3.2 DC-link Voltage Controller

A PI-controller is used as DC-link voltage controller. It is possible to use a PID-controller if increased bandwidth of the control-loop is required. In principle Symmetrical Optimum can be used for tuning the controller. The DC-link capacitor will act similar to the mechanical time constant T_m in the case of speed controller tuning. The output of the PI-controller should be the dc-link inverter current $i_{inv,ref}$, which means that the torque reference value should be calculated as below:

$$c_{dc} \cdot \frac{du_{dc}}{dt} = i_C = i_{dc} - i_{inv} \qquad i_{inv,ref} = \frac{p_{ref}}{u_{dc}} = \frac{n \cdot t_{ref}}{u_{dc}} \quad \Rightarrow \quad t_{ref} = \frac{u_{dc}}{n} \cdot i_{inv,ref}$$

Different approaches can be used for linearizing the control loop. Here, however, the output of the controller is used as torque reference. Please note that t_{ref} has to be negative for positive speed. This means that the sign of speed has to be taken into account when calculating the torque reference.

The dc-link voltage controller was tuned with the SM converter running in dc-link control and the load was applied on the grid side converter as a step. A step load of 80 A, i.e. 0.55 pu, was applied to the grid side converter when the machine was running at 1 pu voltage and the response recorded shows that the undershoot in the dc-link voltage is from 1 pu to 0.988 pu which is equivalent to 1.2 %. The voltage is back to 1 pu within 80 ms as shown in Figure 4.7.

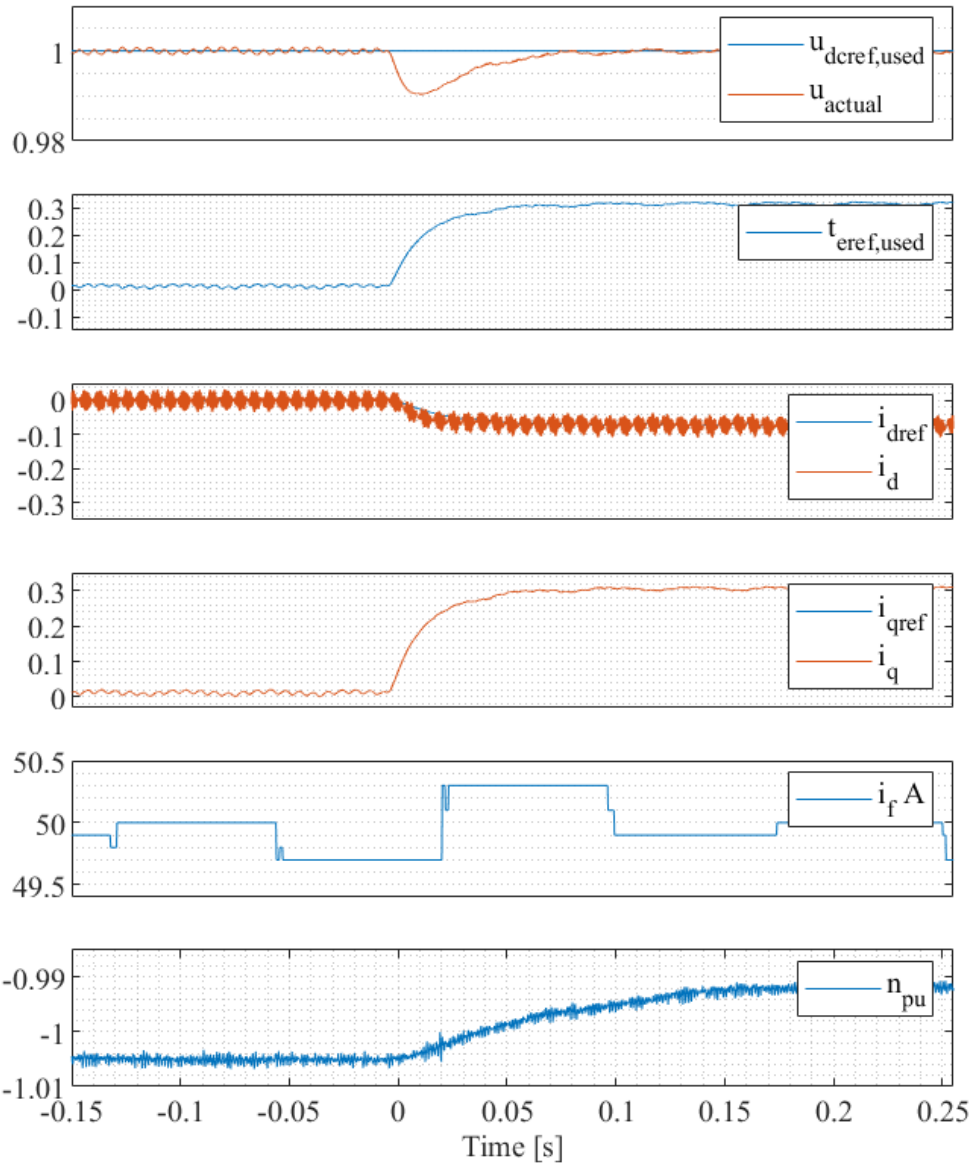

Figure 4.7: SM drive DC-link voltage controller response for 0.55 pu current step in grid converter

5 System Testing

The main target with this sub- project was to develop a synchronous motor drive, which could operate the reversible pump turbine both in turbine- and pump mode. Results from testing and verification of operation of different control loops were presented in the previous chapter. In this chapter tests of the behavior of the drive during start-up, ordinary operation and Low Voltage Ride Through in both turbine and pump mode is presented. Also, the behavior during transition between pump and turbine modes are presented, i.e., Mode Switching.

A typical torque speed characteristic of a reversible pump turbine (RPT) is as shown in Figure 5.1. Please note that in this figure a positive turbine speed is defined as generating mode. Both positive torque and speed gives positive turbine power. This means that the torque equation becomes:

$$J \cdot \frac{d\Omega}{dt} = T_e + T_{turbine}$$

This means that the synchronous machine has to produce a negative torque during steady state operation in both pump and generating mode. For the SM machine motor definitions are used, i.e. the power becomes negative in turbine operation. This means that the SM machine is braking, i.e. generator operation.

The control strategy for pump and turbine operation is as presented in Figure 5.2.

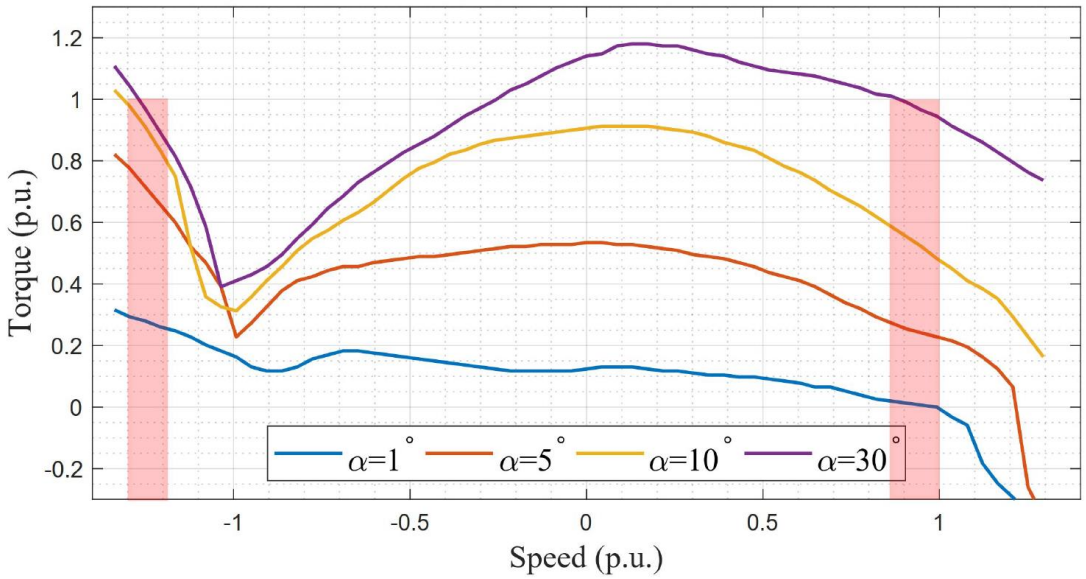

Figure 5.1: Torque speed curves for a Reversible Pump Turbine [5]

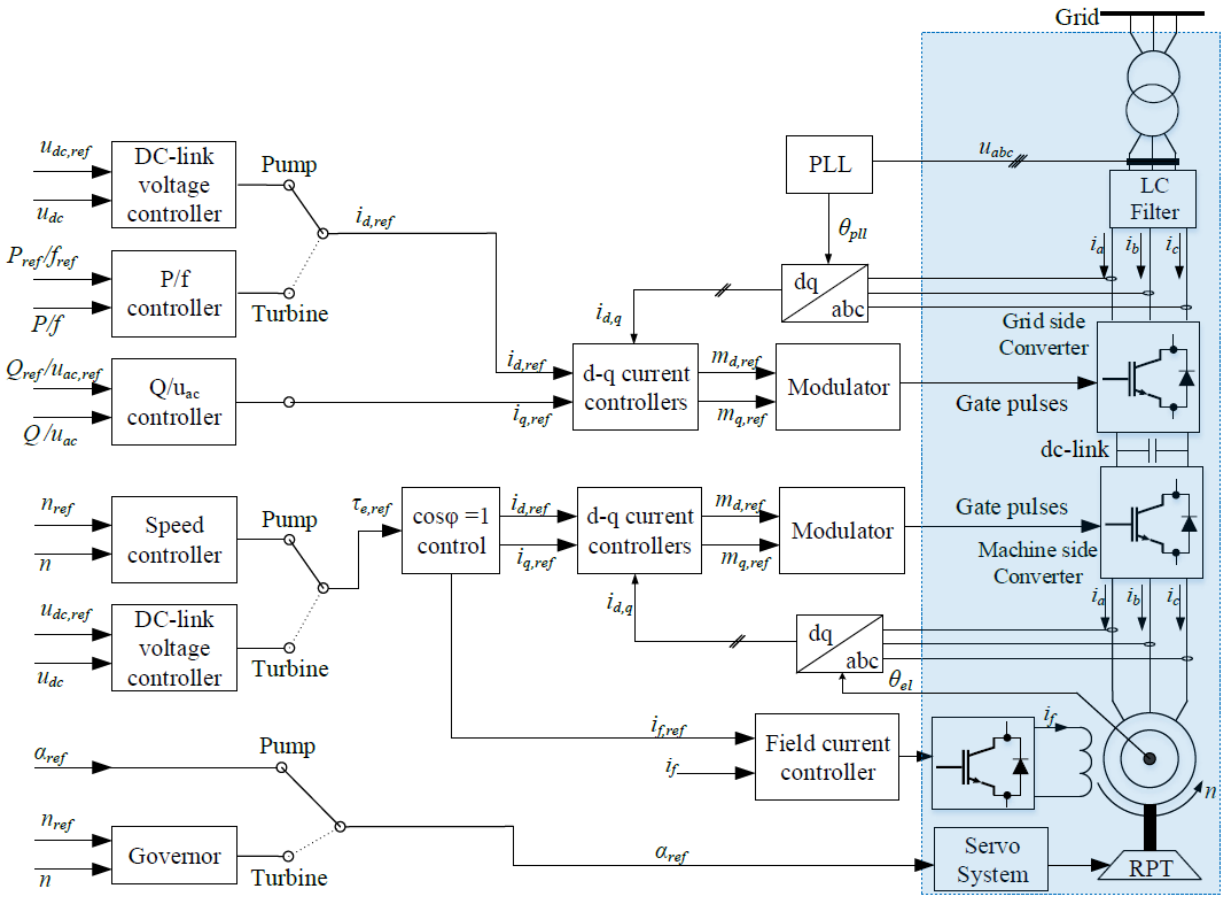

Figure 5.2: The control structure of the RPT drive system [5]

5.1. Pump Mode

First the pump mode will be discussed. The topics are Start Up mode, Ordinary Operation and the Low Voltage Ride Through behavior.

5.1.1 Start Up

In pump mode the SM machine is in speed control mode.

A start-up sequence is presented in Figure 5.3. From t= 0 s to 10 s the SM drive accelerates the system to – 1pu speed. During this period the guide vanes are closed. At t = 12.5 s the guide vanes have started to open and the water flow increases to -0.6 pu. At the = 23.5 s, the speed is further increased to -1.05 pu to increase the water flow, and hence the torque- and power loading of the SM machine. The load changes sharply in this region as expected according to Figure 5.1. The oscillation in the water flow reflects on torque and power of the SM machine. It takes several minutes to stabilize. The system is up running in only a few seconds- The logging is made in Opal RT.

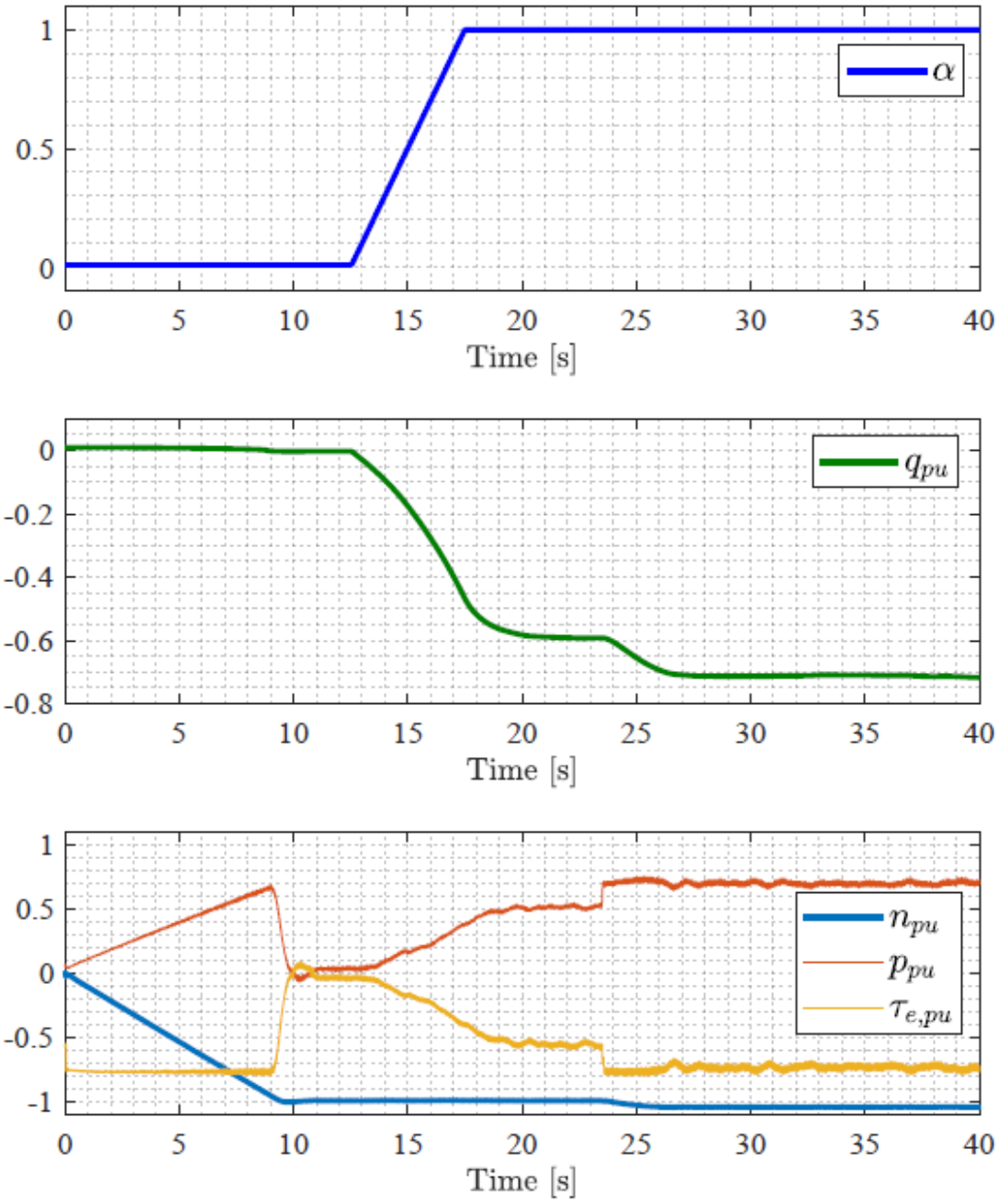

Figure 5.3: Start-up in Pump Mode [5]

5.1.2 Ordinary Operation

In normal operation, the guide vane is kept fully open, and the speed is controlled by the SM converter. The speed of the machine is adjusted to control the water flow in pumping mode. Also, the available pumping power is provided to the secondary controller and the speed is adjusted to follow the power limit.

5.1.3 Low Voltage Ride Through

When there is short circuit at ac terminals, there is no power available for pumping and the speed drops. In practice, the SM torque is limited to zero, due to the DC-link under voltage torque limiter. The whole water column acts against the rotation of the RPT and the speed drops almost linearly. For a mechanical time constant (Tm) of 10 seconds, a short circuit for 0.5 seconds will lead to approx. 5% drop in speed which is within the permissible limit.

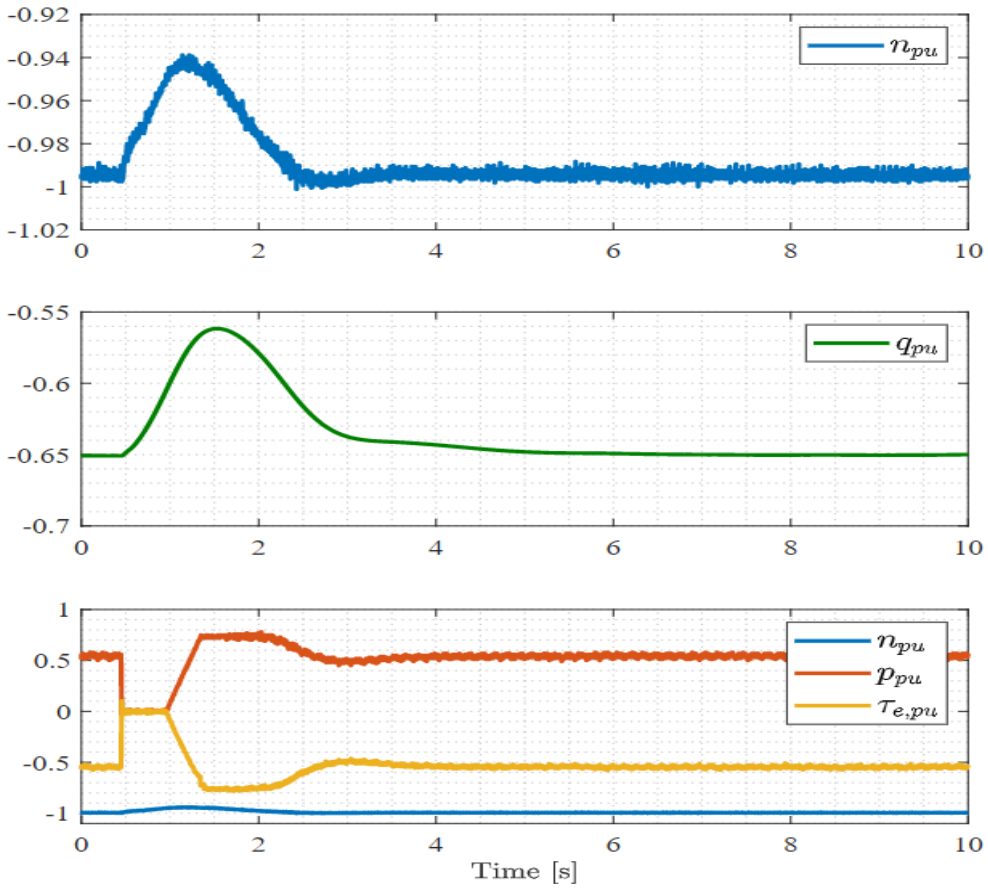

Figure 5.4: Low Voltage Ride Through in Pump Mode

5.2. Turbine Mode

5.2.1 Start Up

In turbine mode the SM machine is in DC-link Voltage control mode.

A start-up sequence is shown in Figure 5.5. First the turbine governor controls the guide vanes α to run the turbine generator set to 1 pu speed. At t= 10 s the machine side converter is started and charging the dc-link capacitor to is reference value. The water flow increases to cover the losses in the turbine, SM machine and machine side converter (inverter). At t= 20 s, the grid side converter is started and synchronized to the grid. At t = 26 s, the power output of -0.25 pu was injected into the grid by controlling the grid-side converter. The recovery of speed takes around 60 seconds, which is acceptable since the grid frequency and turbine speed are decoupled.

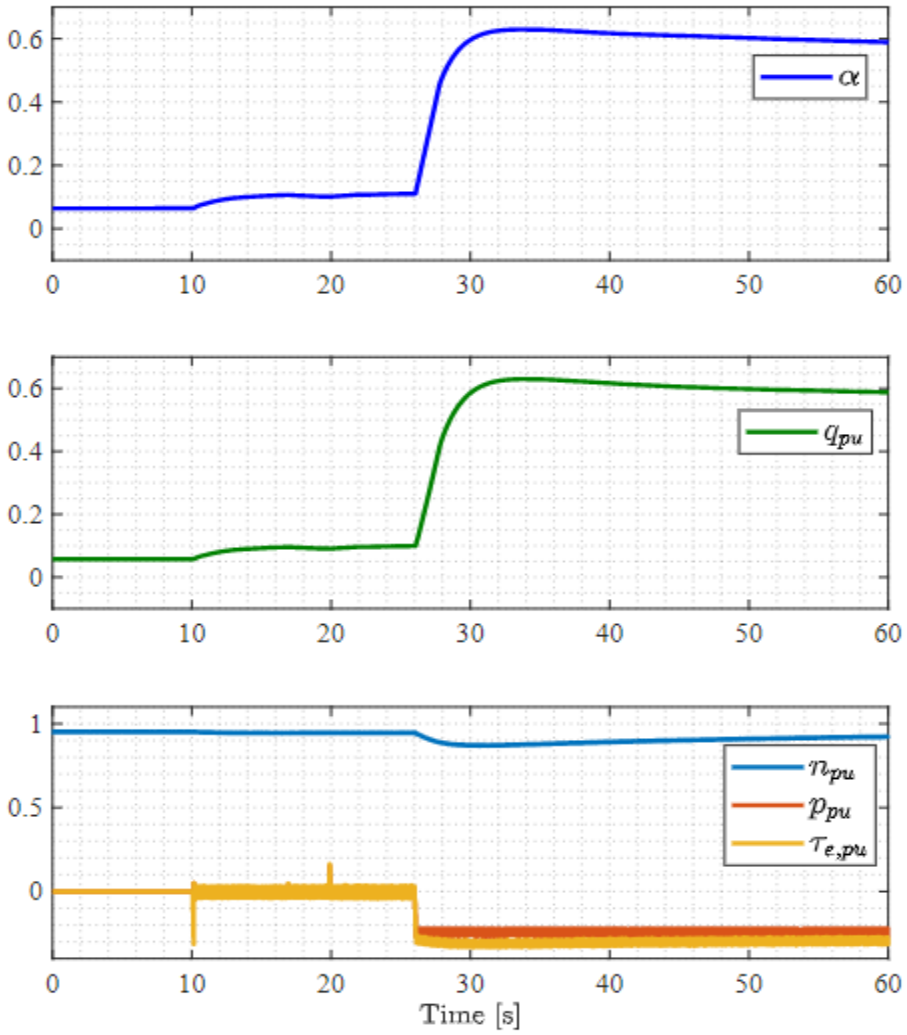

Figure 5.5: Start-up in Turbine Mode [5]

5.2.2 Ordinary Operation

In normal operation, the grid side converter operates in voltage- and frequency droop control mode with the grid and is loaded accordingly. Virtual Inertia and damping can be implemented. The load reflects on the dc-link voltage of the back-to-back converter set and the machine side converter loads the synchronous machine to control the dc-link voltage to the reference value.

5.2.3 Low Voltage Ride Through

The short circuit at AC terminals blocks the power flow from the synchronous machine to the grid. The torque reference will automatically be controlled to zero by the DC-link voltage controller, which leads to rise in the speed of the machine set. But in turbine mode, the governor is still active and therefore, the speed does not rise more than 2 % if the short circuit duration is less than or equal to 0.5s.

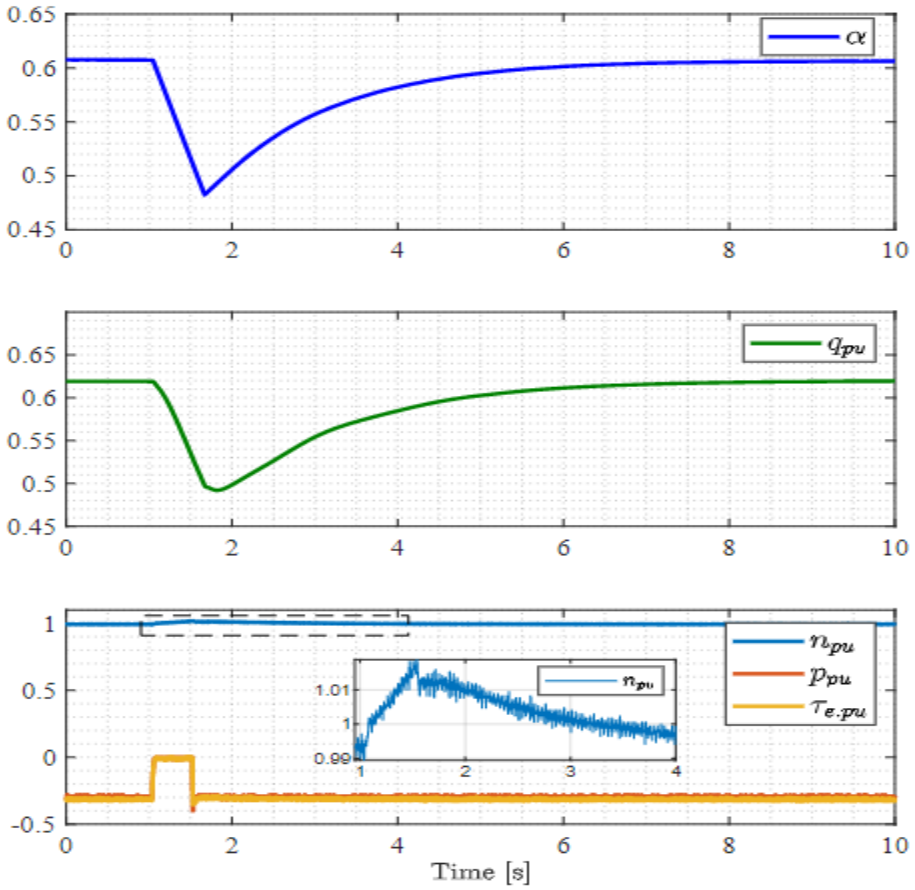

Figure 5.6: Low Voltage Ride Through in Turbine Mode

5.3. Mode Switching

During mode switching it is important that it is the AFE which is in the DC-link Voltage control mode when passing zero speed. The motor drive will at zero speed, not be able to generate power.

5.3.1 Transition from pump to turbine mode

As shown in Figure 5.7, from t = 0 s to t= 13 s the RPT is running in pump mode and the guide vanes have to be closed to initiate the transition of mode from pump- to turbine mode. At t= 13 s, the secondary controller changes the speed reference from -1 to 1 pu to change the speed of the machine to the direction of turbine mode. At t=48 s, the control mode of the SM machine is switched from speed control to dc-link voltage control and at the same time the AFE is switched from dc-link voltage control to voltage- and frequency droop control. At t= 65 s, the machine is loaded using the grid connected AFE.

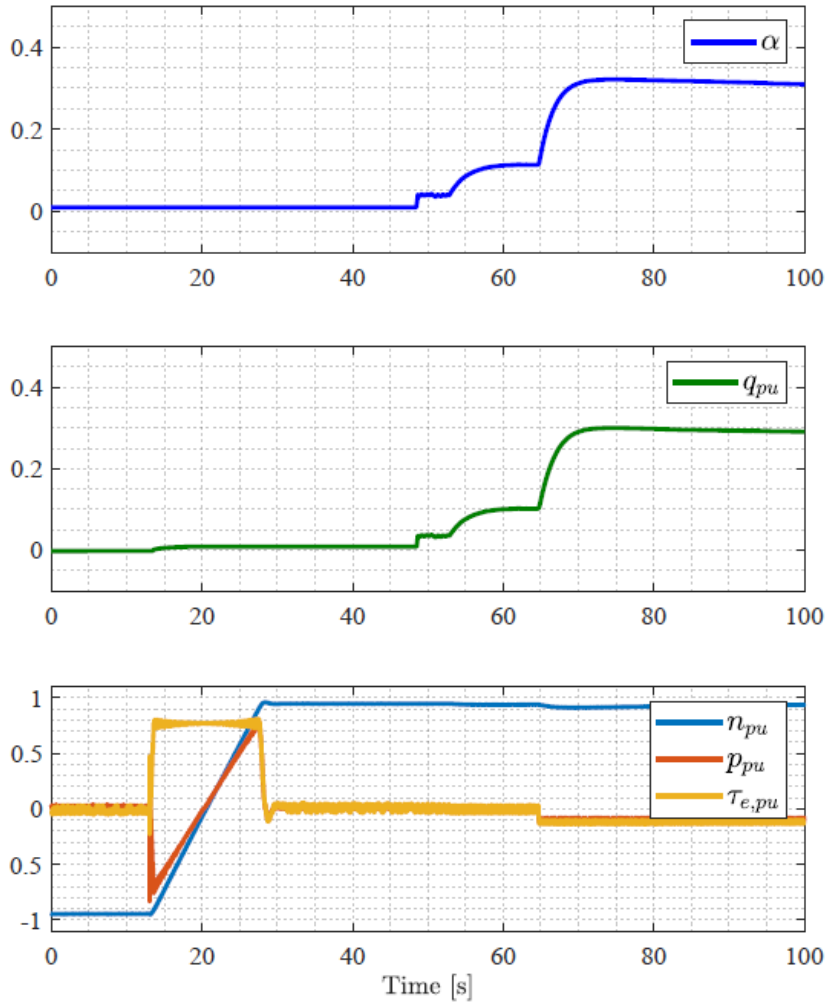

Figure 5.7: Transition from Pump Mode to Turbine Mode

5.3.2 Transition from turbine to pump mode

The transition from turbine to pump mode is shown in Figure 5.8. From t= 0 s to t= 42 s, the RPT is running in turbine mode and the guide vanes are closed to initiate transition from turbine to pump mode. At t= 42 s the control mode of the SM machine is switched from dc-link control mode to speed control. At the same time the grid-side converter is switched from voltage- and frequency droop control to dc-link voltage control mode. At t= 68 s the secondary controller changes the speed reference from 0.5 to -0.93 pu to turn the machine into pump mode direction. At t= 97 s the guide vanes are opened to pump water.

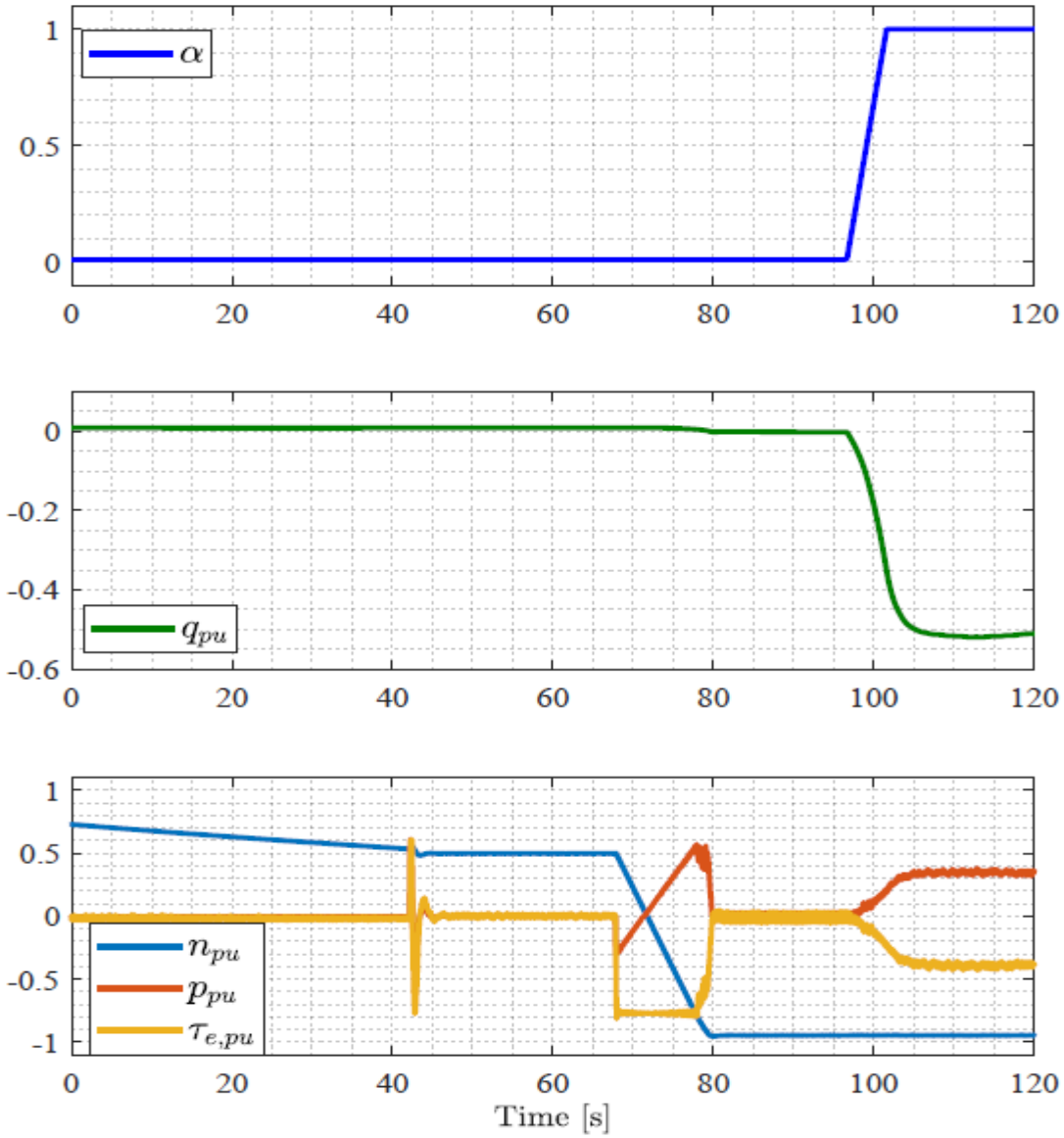

Figure 5.8: Transition from Turbine Mode to Pump Mode

6 Conclusion

A Synchronous Motor Control system has been developed in this HydroFlex project. The process has been divided into 3 steps:

- In the first step, a control system for Synchronous Machines has been devloped by help of the PESC Control Platform, based on a Zynq7030 processor from Xilinx with 2 floating point processors and a Field Programmable Gate Array. The converter, motor and load were emulated in the FPGA together with PWM-modulators and filters. In this way almost the complete SW could be developed and tested succesfully without running the real converters in the lab.
- As a second step, the current controllers, torque control, speed controller and dc-link voltage controllers were tuned/tested on the real 100 kVA set-up in the Smart Grid Lab. The tests were successful and the dynamic behaviors were as expected.
- As a third step, the SM drive was tested together with the Induction Motor Drive running as a Reversible Pump Turbine load emulator. The IM Drive was controlled from the Opal RT. Both pump operation and turbine operation were tested succesfully. Tests including mode switching, i.e. from pump to turbine and from turbine to pump operation, were executed. Even Low Voltage Ride Through was tested.

The conclusion is that the the goals of the project have been accomplished.

Literature/References/Bibliography

[1] Parker, M., Campos-Gaona, D., Anaya-Lara, O.: Intelligent control mechanisms for enhanced fault ride-through performance and provision of ancillary services. HydroFlex Task 4.1: Grid interface and grid code adherence and support

[2] Mo, O.: HydroCen Laboratory setup for real-time emulation of waterways and turbine. SINTEF Energy: D2.1.8 Part II HydroCen Laboratory Setup. 2021-12-20

[3] Ljøkelsøy, K.: Exciter converter for a synchronous generator- Documentation. SINTEF Energy: D2.1.16 Part II AN 20.12.61. Date: 2021-10-14

[4] Bühler, H.R.: Einführung in die Theorie der geregelter Drehstromantriebe. Band 1: Grundlagen. Band 2; Anwendungen. Birkhäuser Verlag, Basel 1977

[5] Tiwari, R., Nilsen, R., Mo, O. : Control Strategies for Variable Speed Operation of Pump Storage Plants with Full-size Converter Fed Synchronous Machines, ECCE-2021